

1    **Complexation of Plutonium(IV) with *trans*-1,2-Diaminocyclohexane-*N,N,N',N'*-tetraacetic**

2    **Acid (CDTA) in Acidic Solution**

3    Mitchell T. Friend,<sup>1</sup> Pihong Zhao,<sup>2</sup> Mavrik Zavarin,<sup>2</sup> and Nathalie A. Wall<sup>\*,1</sup>

4    <sup>1</sup>Department of Chemistry, Washington State University, Pullman, Washington 99164, United  
5    States

6    <sup>2</sup>Glenn T. Seaborg Institute, Physical & Life Sciences, Lawrence Livermore National Laboratory,  
7    Livermore, California 94550, United States

8    \*email: nawall@wsu.edu

9    Keywords: Plutonium(IV), CDTA, Complexation, Stability Constant, Liquid-Liquid Extraction,  
10   Specific ion Interaction Theory

11   **Abbreviations and Symbols**

ALSEP	Actinide Lanthanide Separation
CDTA	<i>trans</i> -1,2-diaminocyclohexane- <i>N,N,N',N'</i> -tetraacetic acid
EDTA	ethylenediamine- <i>N,N,N',N'</i> -tetraacetic acid
GANEX	Group Actinide Extraction
KHP	potassium hydrogen phthalate
PMBP	1-phenyl-3-methyl-4-benzoyl-2-pyrazolin-5-one
SIT	Specific ion Interaction Theory
TRU	transuranic
TTA	2-thenoyltrifluoroacetone
$\beta_{mhx}$	Stability constant of metal-ligand complex M:H:L
$\beta_x^{\text{app}}$	Apparent stability constant
$\beta_{m-h0}$	Hydrolysis constant
$K_a$	Stepwise acid dissociation constant
$K_w$	Autoprotolysis constant of water
$K_{\text{ex}}$	Extraction equilibrium constant
$D_0$	Distribution ratio in the absence of aqueous complexing ligand
$D$	Distribution ratio in the presence of aqueous complexing ligand
$R$	Gas constant (8.3145 J·mol <sup>-1</sup> ·K <sup>-1</sup> )

$T$	Temperature (°C or K)
$F$	Faraday constant (96,485 C·mol <sup>-1</sup> )
$E^\circ$	Standard electrode potential (V)
$E$	Measured electrode potential (V)
$E_j$	Electrode junction potential (V)
$C_i$	Analytical concentration (mol·L <sup>-1</sup> ) of species $i$
$I, I_m$	Ionic strength in molarity (mol·L <sup>-1</sup> ) and molality (mol·kg <sup>-1</sup> )
$K_C, K_m$	Equilibrium constant on the molar and molal scale
$a_{\text{H}_2\text{O}}$	Activity of water
$\gamma_i$	Activity coefficient of species $i$
$\nu_i$	Stoichiometric coefficient of species $i$
$z_i$	Charge of species $i$
$\Delta\epsilon$	Specific ion Interaction Theory (SIT) parameter (kg·mol <sup>-1</sup> )
$\vartheta$	Conversion ratio between molarity (mol·L <sup>-1</sup> ) and molality (mol·kg <sup>-1</sup> )

12

13 **Abstract**

14 Understanding the interaction of Pu(IV) with complexing agents present in the nuclear fuel  
 15 cycle is important for predicting the performance of used nuclear fuel separations. The  
 16 complexation of Pu(IV) with *trans*-1,2-diaminocyclohexane-*N,N,N',N'*-tetraacetic acid (CDTA)  
 17 was studied in acidic solutions of 0.10-0.50 mol·L<sup>-1</sup> HClO<sub>4</sub> with 1.00 mol·L<sup>-1</sup> (Na<sub>2</sub>H)ClO<sub>4</sub> total  
 18 ionic strength by a liquid-liquid extraction method using tracer quantities of <sup>238</sup>Pu. The acid  
 19 dissociation constants of CDTA and the autoprotolysis constant of water were determined via  
 20 potentiometric titrations in 0.10-2.00 mol·L<sup>-1</sup> NaClO<sub>4</sub> and 25.0 ± 0.1 °C. The variation of the  
 21 dissociation constants with ionic strength was modeled with the Specific ion Interaction Theory  
 22 (SIT) and the associated SIT parameters were obtained. The thermodynamic dissociation  
 23 constants at zero ionic strength for water and CDTA were determined from this analysis as  
 24  $pK_w^\circ = 14.00 \pm 0.03$ ,  $pK_{a2}^\circ = 1.52 \pm 0.04$ ,  $pK_{a3}^\circ = 2.78 \pm 0.05$ ,  $pK_{a4}^\circ = 4.17 \pm 0.04$ ,  
 25  $pK_{a5}^\circ = 6.75 \pm 0.02$ , and  $pK_{a6}^\circ = 10.64 \pm 0.04$  at 25.0 ± 0.1 °C. The results of the liquid-liquid  
 26 extraction experiments indicated the formation of a 1:0:1 complex, PuCDTA<sup>0</sup>, and the presence of

27 additional protonated species,  $\text{Pu}(\text{HCDTA})^+$  and  $\text{Pu}(\text{H}_2\text{CDTA})^{2+}$ , at these acidities. The  
28 corresponding stability constants in  $1.00 \text{ mol}\cdot\text{L}^{-1}$   $(\text{Na},\text{H})\text{ClO}_4$  and  $23 \pm 1 \text{ }^\circ\text{C}$  were determined to  
29 be  $\log_{10} \beta_{101} = 24.2 \pm 0.3$ ,  $\log_{10} \beta_{111} = 25.4 \pm 0.2$ , and  $\log_{10} \beta_{121} = 25.8 \pm 0.1$ .

30 **1 Introduction**

31 Nuclear waste management can be improved with used nuclear fuel reprocessing. Fissile  
32 U and Pu, which can represent about 97% of the mass of the used nuclear fuel, may be recovered  
33 and recycled back into the nuclear fuel cycle and used for further energy production. Additional  
34 separations allow for partitioning the remaining long-lived transuranic (TRU) elements from the  
35 relatively short-lived fission products, while TRU elements can be eliminated in fast neutron  
36 reactors by fission or transmutation to short half-life isotopes [1-5]. Such separations reduce the  
37 volume, radiotoxicity, and the thermal load of nuclear waste that will eventually be disposed of in  
38 a geological repository.

39 Reprocessing of used nuclear fuel is accomplished primarily using liquid-liquid extraction  
40 methods. In these systems, complexing agents with an affinity for specific elements are added to  
41 improve separation factors, as is the case for separation of trivalent actinides from lanthanides.  
42 The use of *trans*-1,2-diaminocyclohexane-*N,N,N',N'*-tetraacetic acid (CDTA) has been suggested  
43 in the Actinide Lanthanide Separation (ALSEP) and Group Actinide Extraction (GANEX)  
44 processes to prevent the coextraction of the fission products Zr and Pd with the targeted actinide  
45 elements [1, 5, 6]. Thus, understanding Pu(IV) complexation with CDTA is of importance from  
46 the standpoint of predicting Pu behavior in processes such as ALSEP and GANEX.

47 The chemical structure of CDTA (Fig. 1) is closely related to that of  
48 ethylenediamine-*N,N,N',N'*-tetraacetic acid (EDTA), the difference being a cyclohexane ring in

49 CDTA replacing the ethylene group found in EDTA. The consequence of this cyclohexane ring  
50 makes CDTA have a more rigid structure compared to EDTA and alters the thermodynamics of  
51 complexation with metal cations. While a few studies have reported stability constants for Pu(IV)  
52 with EDTA, and one study is available for Pu(III) with CDTA, no thermodynamic data are  
53 available for the complexation of Pu(IV) with CDTA [7-13]. Additionally, the acid dissociation  
54 constants of CDTA have only been reported at a few different ionic strengths, with no attempt to  
55 describe the ionic strength dependence of the protonation reactions. Modeling the ionic strength  
56 dependence of these equilibrium constants would allow for the extrapolation of their values to  
57 other ionic strengths, providing more accurate parameters for predicting speciation were data  
58 might not be available.

59 This work reports information for the complexation of Pu(IV) with CDTA, including the  
60 determination of the corresponding stability constants in  $\text{NaClO}_4$  media. The complexation of  
61 Pu(IV) with CDTA and the associated thermodynamic data of the complex(es) had not been  
62 quantified, and this work results in the identification of new Pu(IV)-CDTA complexes and  
63 speciation information that is necessary for understanding Pu(IV)-CDTA behavior in advanced  
64 nuclear fuel reprocessing systems. Measurement of CDTA acid dissociation constants were  
65 performed using potentiometry at ionic strengths of  $0.10\text{-}2.00 \text{ mol}\cdot\text{L}^{-1}$   $\text{NaClO}_4$ , and the ionic  
66 strength dependence described with the Specific ion Interaction Theory. A liquid-liquid extraction  
67 method was used to determine the stability constants of Pu(IV)-CDTA in  $1.00 \text{ mol}\cdot\text{L}^{-1}$   
68  $(\text{Na},\text{H})\text{ClO}_4$ . The Pu(IV)-CDTA complexation studies were carried out with tracer concentrations  
69 of  $^{238}\text{Pu}$  in acidic solutions to minimize hydrolysis, colloid formation, and disproportionation of  
70 Pu(IV).

71 **2 Experimental**

72 2.1 Materials

73 All chemicals were reagent grade and used without further purification unless specified  
74 and are listed in Table 1. Aqueous solutions were prepared with distilled, deionized water  
75 (Millipore Synergy,  $18.2 \text{ M}\Omega\cdot\text{cm}^{-1}$ ). Anhydrous  $\text{NaClO}_4$  (98.0-102.0%, ACS certified, Alfa  
76 Aesar) or the monohydrate ( $\geq 99.0\%$ , HPLC grade, Fluka Analytical), potassium hydrogen  
77 phthalate (KHP) (99+%, Acros Organics), and  
78 *trans*-1,2-diaminocyclohexane-*N,N,N',N'*-tetraacetic acid monohydrate ( $\text{H}_4\text{CDTA}\cdot\text{H}_2\text{O}$ )  
79 ( $> 99.0\%$ , TCI) were dried in an oven at  $110^\circ\text{C}$  for 1 hr followed by cooling in a desiccator.  
80 Sodium perchlorate and  $\text{NaNO}_2$  (99.6%, ACS certified, Baker Analyzed) solutions were made by  
81 dissolving a weighed amount of reagent in water. A solution of 50 wt %  $\text{NaOH}$  (pellets,  $\geq 97.0\%$ ,  
82 ACS certified, Fisher) was produced from which carbonate was allowed to precipitate overnight.  
83 Dilutions of  $\text{NaOH}$  were made from this solution with an appropriate amount of  $\text{NaClO}_4$  to fix the  
84 ionic strength, and then standardized by titrations of KHP to a phenolphthalein endpoint using a  
85 Brinkmann Metrohm 765 Dosimat. Carbonate content in the  $\text{NaOH}$  solutions was estimated from  
86 the protolytic impurity level obtained from analyzing the Gran titrations in the program GLEE  
87 (Protonic Software) (a protolytic impurity level  $< 2\%$  was desired), and as such, it was found  
88 necessary to replace these solutions on a weekly basis [14, 15]. Stock solutions of  $\text{HClO}_4$  were  
89 prepared from dilutions of 70% perchloric acid (redistilled, Alfa Aesar) in  $\text{NaClO}_4$  solution of  
90 desired ionic strength and standardized against standardized  $\text{NaOH}$ . Solutions of  
91  $5.00 \times 10^{-3} \text{ mol}\cdot\text{L}^{-1}$  CDTA were prepared by adding weighed portions of the dried reagent to  
92  $\text{NaClO}_4$  solution of appropriate ionic strength, and then adding approximately one mole ratio of  
93 standardized  $\text{NaOH}$  to the CDTA suspension under gentle heating to completely dissolve before  
94 dilution to the final volume. 2-Thenoyltrifluoroacetone (TTA) (99%, Aldrich) was dissolved in

95 *p*-xylene (99%, Acros) to obtain a  $0.100 \text{ mol}\cdot\text{L}^{-1}$  TTA stock solution. This solution was protected  
96 from light and stored in a covered glass bottle when not in use.

97 2.2 Pu(IV) Stock Solution

98 A  $^{238}\text{Pu}(\text{IV})$  stock of  $6 \times 10^{-7} \text{ mol}\cdot\text{L}^{-1}$  total Pu in  $1 \text{ mol}\cdot\text{L}^{-1}$  HCl was used. The isotopic  
99 composition was verified by  $\alpha$ -spectroscopy and liquid scintillation counting as  $99.5 \pm 0.4\% \text{ }^{238}\text{Pu}$   
100 and  $0.5 \pm 0.4\% \text{ }^{239+240}\text{Pu}$  by activity percent. The stock was previously purified (within one year)  
101 and adjusted to Pu(IV) by anion exchange as previously described [16, 17]. Specifically, 2 mL of  
102 Pu in  $8 \text{ mol}\cdot\text{L}^{-1}$   $\text{HNO}_3$  was adjusted to Pu(IV) by adding 100  $\mu\text{L}$  of saturated  $\text{NaNO}_2$  and then  
103 loaded onto a column containing 2 mL of Bio Rad AG 1-X8 (100-200 mesh) anion exchange resin.  
104 The column was rinsed with 3 bed volumes of  $8 \text{ mol}\cdot\text{L}^{-1}$   $\text{HNO}_3$  and then Pu was eluted as Pu(III)  
105 with 15 vol % HI/HCl. A few drops of concentrated  $\text{HNO}_3$  were added to the eluent and heated  
106 to near dryness multiple times to remove HI and oxidize Pu back to Pu(IV), before final dissolution  
107 in  $1 \text{ mol}\cdot\text{L}^{-1}$  HCl. The Pu oxidation state was verified by a liquid-liquid extraction method using  
108  $0.025 \text{ mol}\cdot\text{L}^{-1}$  1-phenyl-3-methyl-4-benzoyl-2-pyrazolin-5-one (PMBP) (99%, Aldrich) in  
109 *p*-xylene which quantitatively extracts only the 4+ oxidation state from  $1 \text{ mol}\cdot\text{L}^{-1}$  HCl [18, 19].  
110 The results from this extraction indicated that the stock was  $96 \pm 2\% \text{ Pu(IV)}$ .

111 2.3 Potentiometric Titration

112 Potentiometric titrations for the quantification of the acid dissociation constants,  $\text{p}K_{\text{a}}$ , of  
113 CDTA were performed with a Mettler Toledo Titration Excellence T50 autotitrator equipped with  
114 a Mettler Toledo DGi111-SC combination glass electrode, Mettler Toledo DT1000 temperature  
115 probe, Mettler Toledo compact propeller stirrer, and controlled with LabX 2016 software (Mettler  
116 Toledo, version 7.0.0). The inner fill solution of the glass electrode was replaced with  $3 \text{ mol}\cdot\text{L}^{-1}$

117 NaCl to avoid precipitation of  $\text{KClO}_4$  in the electrode frit. All titrations were performed under an  
118 argon atmosphere (Ar was bubbled through solutions of  $1 \text{ mol}\cdot\text{L}^{-1}$  NaOH and water to remove  
119  $\text{CO}_2$  and to hydrate the gas) in a 100 mL water-jacketed titration cell connected to an external  
120 circulating water bath (Fisher Scientific Isotemp 3016D). Volumetric pipettes for transferring  
121 solution into the titration cell were calibrated daily by weighing dispensed volumes of water. The  
122 circulating water bath temperature was adjusted such that the temperature of the solution in the  
123 titration cell was maintained at  $25.0 \pm 0.1 \text{ }^\circ\text{C}$  as confirmed by the temperature probe. Typically,  
124 this required setting the bath temperature to 25.1 or 25.2  $^\circ\text{C}$ . At least 100 data points were  
125 collected for each titration curve with a 30 second equilibration time between each addition of  
126 titrant. The volume of titrant dispensed in each addition was adjusted such that the titration  
127 concluded within 1 hr to minimize potential variations due to electrode drift. The glass electrode  
128 was calibrated to give  $\text{p}C_{\text{H}}$  ( $= -\log_{10} [\text{H}^+]$ ) via Gran titrations at each ionic strength [20]. A  
129 2.000 mL aliquot of standardized  $0.1000 \text{ mol}\cdot\text{L}^{-1}$   $\text{HClO}_4$  was added to 50.00 mL of  $\text{NaClO}_4$   
130 solution and titrated with standardized  $0.1000 \text{ mol}\cdot\text{L}^{-1}$  NaOH/ $\text{NaClO}_4$  of the same ionic strength.  
131 The Gran titration data was analyzed in the program GLEE (Protonic Software) for determination  
132 of the standard electrode potential and the electrode slope factor using data from the acidic  
133 ( $\text{p}C_{\text{H}}$  2.5-3.2) and basic ( $\text{p}C_{\text{H}}$  10.8-11.3) regions of the strong acid-base titration curves [14, 15].  
134 The potential readings obtained from these titrations were first used to calculate the value of  $\text{p}K_{\text{w}}$   
135 at each ionic strength and were subsequently used in the Gran analysis to define the relationship  
136 between electrode potential and  $\text{p}C_{\text{H}}$ . Accurate  $\text{p}K_{\text{w}}$  values are crucial to obtain accurate  $\text{p}K_{\text{a}}$   
137 values. The slope factors ranged from 58.72 to 59.30 mV over the course of this work were within  
138 1% of the Nernstian value. A Gran titration was performed before every replicate CDTA titration  
139 to account for any drift in electrode response between runs. Determination of the  $\text{p}K_{\text{a}}$  values of

140 CDTA in  $0.10\text{-}2.00 \text{ mol}\cdot\text{L}^{-1}$   $\text{NaClO}_4$  were performed by acidifying 50.00 mL of  
141  $5.00 \times 10^{-3} \text{ mol}\cdot\text{L}^{-1}$  CDTA to ca.  $\text{pH}\ 2$  by adding a known amount of standardized  
142  $0.1000 \text{ mol}\cdot\text{L}^{-1}$   $\text{HClO}_4/\text{NaClO}_4$ , and then titrating with standardized  $0.1000 \text{ mol}\cdot\text{L}^{-1}$   
143  $\text{NaOH}/\text{NaClO}_4$  of the same ionic strength. Four replicate titrations were performed at each ionic  
144 strength. Fitting of the protonation constants of CDTA was performed in the program  
145 Hyperquad2013 (Protomic Software) [21, 22].

146 2.4 Liquid-Liquid Extraction

147 Liquid-liquid extractions were performed by contacting equal volumes of aqueous and  
148 organic phases (500  $\mu\text{L}$  each) in 1.5 mL screw cap microcentrifuge tubes with at least triplicate  
149 samples for each data point. The samples were vigorously shaken to emulsion on a vortex mixer  
150 for 30 min at room temperature ( $23 \pm 1^\circ\text{C}$ ); preliminary experiments indicated this was sufficient  
151 shaking time to reach extraction equilibrium (Fig. S1, supplementary material). After mixing, the  
152 phases were separated by centrifuging for 1 min at 5000 rpm, and an aliquot of 200  $\mu\text{L}$  from each  
153 phase was then mixed with 5 mL of Perkin Elmer Ultima Gold<sup>TM</sup> LLT liquid scintillation cocktail  
154 and counted on a Perkin Elmer Tri-Carb 2900 TR liquid scintillation analyzer. An energy window  
155 of 100-2000 keV was used, with sample count times of 30 min, or until a 1% error ( $\pm 2\sigma$ ) in the  
156 count rate was achieved. Backgrounds were typically 6-7 cpm.

157 Slope-analysis experiments were performed to elucidate the TTA and  $\text{H}^+$  stoichiometries  
158 of the extracted Pu(IV)-TTA species. The TTA dependence was determined by contacting varied  
159 concentrations of TTA ( $0.010\text{-}0.050 \text{ mol}\cdot\text{L}^{-1}$ ) in *p*-xylene with aqueous solutions of ca.  
160 11,000 cpm  $^{238}\text{Pu}$  (ca.  $6 \times 10^{-9} \text{ mol}\cdot\text{L}^{-1}$  total Pu(IV)) in  $1.00 \text{ mol}\cdot\text{L}^{-1}$   $\text{HClO}_4$  and  $1 \times 10^{-3} \text{ mol}\cdot\text{L}^{-1}$   
161  $\text{NaNO}_2$  to maintain Pu in the 4+ oxidation state. To determine the  $\text{H}^+$  dependence, a constant  
162 concentration of  $0.030 \text{ mol}\cdot\text{L}^{-1}$  TTA in *p*-xylene was used, varying the concentration of

163 standardized  $\text{HClO}_4$  in the aqueous phase from 0.75 to 1.00  $\text{mol}\cdot\text{L}^{-1}$  with the addition of  $\text{NaClO}_4$   
164 to maintain the ionic strength at 1.00  $\text{mol}\cdot\text{L}^{-1}$ . To determine the  $\text{Pu(IV)}$ -CDTA stability constants,  
165 ca.  $6 \times 10^{-9}$   $\text{mol}\cdot\text{L}^{-1}$  total  $\text{Pu(IV)}$  and varied concentrations of CDTA (0 to  $1.00 \times 10^{-3}$   $\text{mol}\cdot\text{L}^{-1}$ )  
166 were added to the aqueous phase with 0.020  $\text{mol}\cdot\text{L}^{-1}$  TTA in the *p*-xylene organic phase. These  
167 experiments were performed at different concentrations of standardized  $\text{HClO}_4$  from 0.10 to  
168 0.50  $\text{mol}\cdot\text{L}^{-1}$  (there was no complexation between  $\text{Pu(IV)}$  and CDTA observed at  $> 0.50 \text{ mol}\cdot\text{L}^{-1}$   
169  $\text{HClO}_4$ ) while maintaining the ionic strength at 1.00  $\text{mol}\cdot\text{L}^{-1}$  with  $\text{NaClO}_4$  at room temperature  
170 ( $23 \pm 1$   $^{\circ}\text{C}$ ).

171 **3 Results and Discussion**

172 **3.1 Measurement of  $\text{p}K_w$**

173 The electrode potential readings obtained over the course of the Gran titrations were used  
174 to calculate the autoprotolysis constant of water,  $\text{p}K_w$ , in solutions of 0.10-2.00  $\text{mol}\cdot\text{L}^{-1}$   
175  $\text{NaClO}_4$  [23-26]. Accurate  $\text{p}K_w$  values are crucial to obtain accurate  $\text{p}K_a$  values. During the  
176 titration of a strong acid with a strong base, the measured electrode potential in the acidic region  
177 (before the equivalence point) of the titration curve can be written as:

$$E = E^\circ + \ln(10) \frac{RT}{F} \log_{10} [\text{H}^+] \gamma_{\text{H}^+} + E_j \quad (1)$$

178 where  $E$  is the measured electrode potential,  $E^\circ$  is the standard electrode potential,  $R$  is the gas  
179 constant,  $T$  is the absolute temperature,  $F$  is the Faraday constant,  $\gamma_{\text{H}^+}$  is the activity coefficient of  
180  $\text{H}^+$ , and  $E_j$  is the junction potential. At constant ionic strength, the activity coefficients and the  
181 junction potential are constants, and can be combined into the standard electrode potential to  
182 provide a new constant,  $E^\circ'$ , which at 25  $^{\circ}\text{C}$  is:

$$\begin{aligned}
 E &= E^\circ + (59.16 \text{ mV}) \log_{10} [\text{H}^+] \\
 &= E^\circ - (59.16 \text{ mV}) \text{p}C_{\text{H}}
 \end{aligned} \tag{2}$$

183 Following a similar argument, the electrode potential response in the basic region of the titration  
 184 curve can be written:

$$\begin{aligned}
 E &= E^\circ + \ln(10) \frac{RT}{F} \log_{10} \left( \frac{K_w}{[\text{OH}^-] \gamma_{\text{OH}}} \right) + E_j \\
 &= E^\circ - (59.16 \text{ mV}) \text{p}K_w + (59.16 \text{ mV}) \text{p}C_{\text{OH}}
 \end{aligned} \tag{3}$$

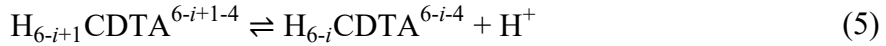
185 Plots of  $E$  vs.  $\text{p}C_{\text{H}}$  in the acidic region, or vs.  $\text{p}C_{\text{OH}}$  in the basic region, have  $y$ -intercepts of  
 186  $E_a^\circ = E^\circ$  (Eq. 2) and  $E_b^\circ = E^\circ - (59.16 \text{ mV}) \text{p}K_w$  (Eq. 3) respectively. The  $\text{p}C_{\text{H}}$  in the acidic  
 187 region and the  $\text{p}C_{\text{OH}}$  in the basic region are calculated from the known amounts of standardized  
 188 strong acid or from the excess standardized strong base added during the titration. The value of  
 189  $\text{p}K_w$  is determined from  $E_a^\circ$  and  $E_b^\circ$ :

$$\text{p}K_w = \frac{E_a^\circ - E_b^\circ}{59.16 \text{ mV}} \tag{4}$$

190 Titration data from at least four Gran titrations at each ionic strength were generated (Fig. 2) to  
 191 determine  $E_a^\circ$  and  $E_b^\circ$ , and Eq. 4 was used to calculate  $\text{p}K_w$ . The averaged values of the obtained  
 192  $\text{p}K_w$  values are presented with Table 2 with errors corresponding to  $\pm 3\sigma$  from quadruplicate  
 193 titrations. Our reported values agree well with those in the literature in  $\text{NaClO}_4$  media, and there  
 194 is an exceptional agreement with the values reported in the NIST stability constant  
 195 database [27-31]. However, a slight discrepancy was observed between the NIST value of  
 196  $13.95 \pm 0.01$  in  $2.00 \text{ mol}\cdot\text{L}^{-1} \text{NaClO}_4$ , which was higher than our value of  $13.87 \pm 0.03$  but still  
 197 agree within 1%. Our experimentally determined  $\text{p}K_w$  values were used for the analysis of the  
 198 Gran titration curves for electrode calibration and when refining the CDTA  $\text{p}K_a$  values.

## 199 3.2 CDTA Acid Dissociation Constants

200 The acid dissociation constants of CDTA were determined in ionic strengths of  
 201 0.10-2.00 mol·L<sup>-1</sup> NaClO<sub>4</sub> via potentiometric titration. CDTA is a hexaprotic, weak acid with  
 202 stepwise acid dissociation constants,  $K_{ai}$ , corresponding to the following equilibrium:



$$K_{ai} = \frac{[\text{H}_{6-i}\text{CDTA}^{6-i-4}][\text{H}^+]}{[\text{H}_{6-i+1-4}\text{CDTA}^{6-i+1-4}]} \quad (6)$$

203 Representative titration curves of CDTA at each ionic strength are displayed in Fig. 3. Fitting the  
 204 titration data in the program Hyperquad2013 from four replicate titrations at each ionic strength  
 205 yielded the values for p $K_{a2}$  through p $K_{a6}$  and are summarized in Table 2 with errors reported as  
 206  $\pm 3\sigma$  from quadruplicate titrations. The speciation of CDTA in 1.00 mol·L<sup>-1</sup> NaClO<sub>4</sub> is presented  
 207 in Fig. S2 in the supplementary material. The values reported in the NIST database are only listed  
 208 in ionic media of Na<sup>+</sup> salts and only a few additional references report these values specifically in  
 209 NaClO<sub>4</sub> [27, 32-34]. Our results in 0.50 and 1.00 mol·L<sup>-1</sup> NaClO<sub>4</sub> are in good agreement with the  
 210 corresponding conditions by Chinea et al. [32] and Anderegg [33]. At an ionic strength of  
 211 0.10 mol·L<sup>-1</sup>, the NIST database provides values for p $K_{a3}$ , p $K_{a4}$ , and p $K_{a5}$  only. No previously  
 212 reported values at 2.00 mol·L<sup>-1</sup> ionic strength were identified. Attempts to include p $K_{a1}$  in the data  
 213 fitting resulted in a failure in refinement, i.e. the free concentrations of every species at each p $C_H$   
 214 could not be calculated. This is explained when considering that the corresponding species  
 215 H<sub>6</sub>CDTA<sup>2+</sup> likely contributes < 1% of the CDTA speciation at p $C_H$  2; the lowest p $C_H$  value in the  
 216 collected titration curves, and thus the mass balance expressions for C<sub>CDTA</sub> and C<sub>H</sub> could not be  
 217 solved when that species was included in the chemical model. Though attempts to measure p $K_{a1}$   
 218 were made using lower starting p $C_H$  (< 2), electrode response suffered due to changes in electrode

219 junction potential which resulted in unacceptable errors. Generally, the electrode junction  
220 potential of a glass electrode varies as a function of  $[H^+]$  and  $\gamma_{H^+}$  at  $pC_H < 2$  and is no longer a  
221 constant term under such conditions. This meant that electrode response was no longer a linear  
222 function of  $pC_H$  alone, and led to large  $|pC_H^{\text{measured}} - pC_H^{\text{calculated}}|^2$  residuals which resulted in high  
223 errors in this region of the titration curves. Indeed, higher errors are also reflected in the values  
224 that were determined for  $pK_{a2}$  which had values  $< 2$ . The only reported values for  $pK_{a1}$  are 0.96  
225 measured by Beck and Görög [33, 35] via solubility experiments in dilute  $HClO_4$  at 20 °C, and  
226 1.09 ± 0.02 in 1 mol·L<sup>-1</sup> KCl at 25 °C by Merciny et al. [13].

227 3.3 SIT Parameters

228 The variation of  $pK_w$  and the CDTA  $pK_a$  values with ionic strength were modeled following  
229 the Specific ion Interaction Theory (SIT) approach [36]. Within the SIT model, the equilibrium  
230 constants are described as a function of ionic strength by:

$$pK_w + \Delta z^2 D + \log_{10} a_{H_2O} = pK_w^\circ + \Delta \varepsilon I_m \quad (7)$$

$$pK_{ai} + \Delta z^2 D = pK_{ai}^\circ + \Delta \varepsilon I_m \quad (8)$$

231 where  $K_w^\circ$  and  $K_{ai}^\circ$  are the thermodynamic equilibrium constants at zero ionic strength,  $a_{H_2O}$  is  
232 the activity of water,  $I_m$  is the ionic strength in molality (mol·kg<sup>-1</sup>),  $D$  is the Debye-Hückel term  
233 equal to  $(0.509 \cdot I_m^{1/2}) / (1 + 1.5 \cdot I_m^{1/2})$  at 25 °C,  $\Delta z^2$  is the change in squared charge over the course  
234 of the reaction given by:

$$\Delta z^2 = \sum (v_i z_i^2)_{\text{products}} - \sum (v_j z_j^2)_{\text{reactants}} \quad (9)$$

235  $\Delta \varepsilon$  is the SIT parameter that is the difference in the individual parameters that describe specific ion  
236 interactions in a given background electrolyte medium:

$$\Delta\epsilon = \sum (v_i \epsilon_i)_{\text{products}} - \sum (v_j \epsilon_j)_{\text{reactants}} \quad (10)$$

237 where  $v$  are stoichiometric coefficients. Tabulated values of  $a_{\text{H}_2\text{O}}$  in various background  
 238 electrolyte media are accessible in the literature [36]. The SIT parameters are determined using  
 239 Eqs. 7 and 8; plots of  $(\text{p}K_w + \Delta\epsilon^2 D + \log_{10} a_{\text{H}_2\text{O}})$  or  $(\text{p}K_{\text{a}i} + \Delta\epsilon^2 D)$  as functions of  $I_m$  produce linear  
 240 relationships with slopes equal to  $\Delta\epsilon$  and  $y$ -intercepts equal to  $\text{p}K_i^\circ$ . Using this approach however,  
 241 requires converting the equilibrium constants on the molar scale ( $K_C$ ) to the molal scale ( $K_m$ )  
 242 by [36]:

$$\text{p}K_m = \text{p}K_C - \sum v_i \log_{10} \vartheta \quad (11)$$

243 where  $\vartheta$  is the ratio between molality and molarity for a given background electrolyte. The value  
 244 of  $\sum v_i$  in the case of the stepwise dissociation constants equals 1. The determined  $\text{p}K_w$  and CDTA  
 245  $\text{p}K_a$  values were converted to the molal scale with Eq. 11 and then the SIT parameters determined  
 246 from the error weighted least squares regression of the SIT plots. These plots are shown in Fig. 4  
 247 and the resulting SIT parameters are displayed in Table 3.

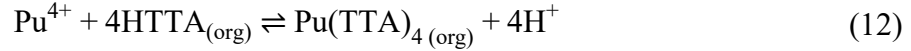
248 The value of  $\text{p}K_w$  decreases with an increasing ionic strength from 0.10 to 0.50 mol·L<sup>-1</sup>  
 249 NaClO<sub>4</sub>;  $\text{p}K_w$  then increases from ionic strength from 0.50 to 2.00 mol·L<sup>-1</sup> NaClO<sub>4</sub>. The resulting  
 250 SIT analysis leads to  $\text{p}K_w^\circ = 14.00 \pm 0.03$  and  $\Delta\epsilon = 0.13 \pm 0.02$  kg·mol<sup>-1</sup>. There is agreement  
 251 between our measured value of  $\text{p}K_w^\circ$  and those reported by NIST and Du et al. [27, 29]. A  
 252 discrepancy in our value of  $\Delta\epsilon$  is observed when compared to the higher value of  
 253  $\Delta\epsilon = 0.1910$  kg·mol<sup>-1</sup> reported by Du et al. The work by Du et al. also utilized potentiometric  
 254 titration to measure  $\text{p}K_a$  values for acetic acid, HF, and  $\text{p}K_w$  at varying ionic strengths of NaClO<sub>4</sub>,  
 255 but the method for calculating  $\text{p}K_w$  from their data was not explicitly stated. However, it is inferred  
 256 that  $\text{p}K_w$  was used as an adjustable fit parameter and obtained from the first derivative analysis of

257  $pK_a$  titrations of acetic acid and HF. Additionally, the changes in  $a_{H_2O}$  with ionic strength was not  
258 included in the SIT model of Du et al. If the  $a_{H_2O}$  term is not included in the SIT fitting of our  
259  $pK_w$  data,  $pK_w^\circ$  remains unchanged but we observed an increase of slope resulting in a higher value  
260 of  $\Delta\epsilon$ . The absence of the contribution of  $a_{H_2O}$  in the SIT model is a likely explanation for why  
261 the value from Du et al. is higher than our result. Finally, Du et al. did not report any error  
262 associated to  $\Delta\epsilon$ , while we report data with a  $\pm 3\sigma$  error; the two results may in fact overlap at the  
263 99% confidence interval.

264 The SIT parameters for the CDTA  $pK_a$  values had not yet been reported in the literature.  
265 The  $pK_a$  values decrease with an increasing ionic strength from 0.10 to 0.50 mol·L<sup>-1</sup> NaClO<sub>4</sub>, and  
266 then increase from 0.50 to 2.00 mol·L<sup>-1</sup> NaClO<sub>4</sub>. An exception to this trend was observed for  $pK_{a4}$   
267 which was found to continuously decrease, i.e. become more acidic, from 0.10 to 2.00 mol·L<sup>-1</sup>  
268 NaClO<sub>4</sub> and is reflected in the SIT parameter as having a negative value,  
269  $\Delta\epsilon_4 = -0.11 \pm 0.03$  kg·mol<sup>-1</sup>. The equilibrium reaction of  $pK_{a4}$  corresponds to the deprotonation  
270 of the final carboxylate group of CDTA. The increasing acidity of this carboxylate group with an  
271 increasing ionic strength maintained by NaClO<sub>4</sub> suggests stronger specific ion interactions  
272 between (Na<sup>+</sup>, H<sub>2</sub>CDTA<sup>2-</sup>) than (H<sup>+</sup>, H<sub>2</sub>CDTA<sup>2-</sup>), thus the increased acidity of that proton. There  
273 is perhaps increasing association/complexation of Na<sup>+</sup> with the fully deprotonated carboxylate  
274 groups that is thermodynamically more favorable than the (likely) rapid isomeric equilibrium of  
275 that proton between the four carboxylate groups of CDTA. Calorimetry experiments or van't Hoff  
276 analysis could be performed to determine if there is an enthalpic or entropic driving force that can  
277 further explain this phenomenon.

278 3.4 Pu(IV)-TTA Extraction Stoichiometry

279 The extraction of Pu(IV) with TTA can be expressed by:



280 with an extraction equilibrium constant,  $K_{\text{ex}}$ :

$$K_{\text{ex}} = \frac{[\text{Pu}(\text{TTA})_4]_{(\text{org})} [\text{H}^+]^4}{[\text{Pu}^{4+}] [\text{HTTA}]_{(\text{org})}^4} \quad (13)$$

281 where HTTA is the enol form of TTA that exchanges  $\text{H}^+$  with the aqueous phase as it extracts a  
282 metal cation into the organic phase [37]. Perchlorate is a weakly complexing anion and  
283 complexation with Pu(IV) is negligible, therefore  $\text{ClO}_4^-$  is not expected to participate in the  
284 extraction equilibrium. The distribution ratio of Pu(IV) is the analytical concentration of Pu(IV)  
285 in the organic phase divided by the analytical concentration of Pu(IV) in the aqueous phase after  
286 extraction and was determined radiometrically by measuring the count rate of  $^{238}\text{Pu}$  in each phase.  
287 Thus, the distribution ratio in the absence of CDTA,  $D_0$ , is expressed as:

$$D_0 = \frac{[\text{Pu}(\text{TTA})_4]_{(\text{org})}}{[\text{Pu}^{4+}] + \sum [\text{Pu}(\text{OH})_h]^{4-h}} = \frac{[\text{Pu}(\text{TTA})_4]_{(\text{org})}}{[\text{Pu}^{4+}] \left( 1 + \sum \beta_{1-h} [\text{H}^+]^h \right)} \quad (14)$$

288 where  $\beta_{1-h}$  are the hydrolysis constants for Pu(IV), taken from Baes and Mesmer which contains  
289 a complete set of Pu(IV) hydrolysis constants at  $1 \text{ mol}\cdot\text{L}^{-1}$   $(\text{Na},\text{H})\text{ClO}_4$  ionic strength [38].  
290 Equation 13 can be written in terms of  $D_0$  by combining with Eq. 14, after which taking the  
291 logarithm yields:

$$\log_{10} \left\{ D_0 \left( 1 + \sum \beta_{1-h} [\text{H}^+]^h \right) \right\} = \log_{10} K_{\text{ex}} + 4 \log_{10} [\text{HTTA}]_{(\text{org})} - 4 \log_{10} [\text{H}^+] \quad (15)$$

292 From Eq. 15, plots of  $\log_{10} \{D_0(1 + \sum \beta_{1-h} [\text{H}^+]^h)\}$  vs.  $\log_{10} [\text{HTTA}]_{(\text{org})}$  or  $\log_{10} [\text{H}^+]$  provide  
293 expected slopes of 4 and -4 respectively based on the expected stoichiometries of TTA and  $\text{H}^+$   
294 given in Eq. 12. The results of these slope-analysis experiments are plotted in Fig. 5 and gave the

295 expected slopes of  $3.9 \pm 0.1$  for the TTA dependence and  $-3.8 \pm 0.2$  for the  $\text{H}^+$  dependence from  
296 the error weighted least squares regression. This indicates that the extraction mechanism in Eq. 12  
297 does indeed describe the extraction of Pu(IV) with TTA and that  $\text{Pu}(\text{TTA})_4$  is the only species  
298 extracted into the organic phase. Additionally, these results verified that Pu remained in the 4+  
299 oxidation state during the extractions; slopes significantly different from 4 would have indicated  
300 reduction or oxidation of Pu(IV) had occurred [39, 40]. This data was also used to calculate the  
301 extraction equilibrium constant with Eq. 15; our results indicate  $\log_{10} K_{\text{ex}} = 6.02 \pm 0.06$   
302 ( $1.00 \text{ mol}\cdot\text{L}^{-1} (\text{Na},\text{H})\text{ClO}_4/p\text{-xylene}/23 \pm 1^\circ\text{C}$ ).

303 Comparing the values of  $K_{\text{ex}}$  for the Pu(IV)-TTA system (Table 4), our value is observed  
304 to be lower than those previously reported in different organic diluents. Values measured in  
305 benzene have been reported in the review article by Poskanzer et al. [41] as  $\log_{10} K_{\text{ex}} = 6.8$   
306 ( $1 \text{ mol}\cdot\text{L}^{-1} \text{ HClO}_4/\text{benzene}$ ) and Ramakrishna et al. [42] report  $\log_{10} K_{\text{ex}} = 7.3$   
307 ( $1.0\text{--}2.0 \text{ mol}\cdot\text{L}^{-1} \text{ HClO}_4/\text{benzene}/25^\circ\text{C}$ ), while values using toluene have been reported by Nash  
308 et al. [43] as  $\log_{10} K_{\text{ex}} = 6.6 \pm 0.1$  ( $2.0 \text{ mol}\cdot\text{L}^{-1} (\text{Na},\text{H})\text{ClO}_4/\text{toluene}/25.0^\circ\text{C}$ ) and by Xia et al. [39,  
309 40] as  $\log_{10} K_{\text{ex}} = 7.08 \pm 0.01$  ( $2.0 \text{ mol}\cdot\text{L}^{-1} \text{ HClO}_4/\text{toluene}/25^\circ\text{C}$ ). No studies using *p*-xylene have  
310 previously been reported and we cannot make a direct comparison. This is of importance because  
311 the extraction of Zr(IV) with TTA in different aliphatic and aromatic diluents from  $1 \text{ mol}\cdot\text{L}^{-1}$   
312  $\text{HNO}_3$  leads to decreasing  $K_{\text{ex}}$  values in aromatic diluents following the trend  
313 benzene>toluene>nitrobenzene [44]. The authors attributed the variation in  $K_{\text{ex}}$  to the changes in  
314 the dielectric constant and dipole moment of the organic phase diluent. This concept also seems  
315 to apply to the Pu(IV)-TTA system, where the  $K_{\text{ex}}$  value varies depending on the diluent used;  
316 appearing to decrease following trend benzene>toluene>*p*-xylene. A potentially linear trend is  
317 observed between  $K_{\text{ex}}$  and the density of the organic diluent decreasing on the order of

318 benzene>toluene>*p*-xylene, however no apparent relationships are observed between  $K_{\text{ex}}$  and other  
 319 solvent parameters such as the dielectric constant or dipole moment of the organic diluent. The  
 320 spread found in the literature  $K_{\text{ex}}$  values, which differ by almost one order of magnitude under the  
 321 same reported experimental conditions, and the limited number of diluents explored make defining  
 322 an analytical trend difficult, and a systematic study of diluent effects on the liquid-liquid extraction  
 323 of Pu(IV) may be warranted.

324 3.5 Pu(IV)-CDTA Complexation

325 The complexation of Pu(IV) with CDTA can be described by the following equilibrium:



326 with a stability constant:

$$\beta_{1hx} = \frac{[\text{Pu}(\text{H}_h\text{CDTA}_x)^{4+h-4x}]}{[\text{Pu}^{4+}]^h [\text{H}^+]^h [\text{CDTA}^{4-}]^x} \quad (17)$$

327 By convention, negative values of  $h$  indicate a hydroxo species. The distribution ratio of Pu(IV)  
 328 in the presence of CDTA in the aqueous phase,  $D$ , is defined:

$$\begin{aligned} D &= \frac{[\text{Pu}(\text{TTA})_4]_{(\text{org})}}{[\text{Pu}^{4+}] + \sum [\text{Pu}(\text{OH})_h^{4-h}] + \sum [\text{Pu}(\text{H}_h\text{CDTA}_x)^{4+h-4x}]} \\ &= \frac{[\text{Pu}(\text{TTA})_4]_{(\text{org})}}{[\text{Pu}^{4+}] \left( 1 + \sum \beta_{1-h0} [\text{H}^+]^{-h} + \sum \beta_{1hx} [\text{H}^+]^h [\text{CDTA}^{4-}]^x \right)} \end{aligned} \quad (18)$$

329 Combining Eqs. 14 and 18 gives:

$$\frac{1}{D} = \frac{1}{D_0} + \sum \frac{\beta_x^{\text{app}}}{D_0} [\text{CDTA}^{4-}]^x \quad (19)$$

330 where  $\beta_x^{\text{app}}$  is an apparent stability constant defined as:

$$\beta_x^{\text{app}} = \frac{\sum \beta_{1hx}}{\left(1 + \sum \beta_{1-h0} [\text{H}^+]^h\right)} [\text{H}^+]^h \quad (20)$$

331 At a fixed  $[\text{H}^+]$ , plots of  $1/D$  against the concentration of free CDTA,  $[\text{CDTA}^{4-}]$ , have a  $y$ -intercept  
 332 proportional to  $D_0$  and coefficients proportional to  $\beta_x^{\text{app}}$ . The distribution ratio was measured  
 333 varying the concentration of CDTA in solutions of standardized 0.10-0.50 mol·L<sup>-1</sup>  $\text{HClO}_4$  with  
 334 1.00 mol·L<sup>-1</sup>  $(\text{Na},\text{H})\text{ClO}_4$  total ionic strength, and then plotted according to Eq. 19. The  
 335 concentration of free CDTA was calculated at each  $[\text{H}^+]$  using our measured  $\text{p}K_a$  values and the  
 336 value of  $\text{p}K_{a1} = 0.96$  from Beck and Görög at 1.00 mol·L<sup>-1</sup>  $\text{NaClO}_4$  ionic strength [33, 35]. The  
 337 distribution data was found to follow a linear trend with respect to  $1/D$  vs.  $[\text{CDTA}^{4-}]$  at each  $[\text{H}^+]$   
 338 and fit with error weighted least squares. Representative plots are shown in Fig. 6 and the  
 339 distribution data can be found in the supplementary material (Tables S1-S5). The linear fits of  $1/D$   
 340 vs.  $[\text{CDTA}^{4-}]$  indicate a Pu(IV)-CDTA stoichiometry of 1:1, i.e.  $x = 1$ , and the  $\beta^{\text{app}}$  values were  
 341 obtained from the slopes of the linear regression at each  $[\text{H}^+]$  according to Eq. 19. If no protonated  
 342 Pu(IV)-CDTA complexes are present, there should be little variation in the values of  $\beta^{\text{app}}$  with  
 343 changes in acidity. However, the measured  $\beta^{\text{app}}$  values (Table S6) were found to increase in  
 344 magnitude with increasing  $[\text{H}^+]$ , indicating the formation of one or more protonated Pu(IV)-CDTA  
 345 species. The plot of  $\beta^{\text{app}}$  vs.  $[\text{H}^+]$  in Fig. 7 followed 2<sup>nd</sup>-order polynomial behavior, implying the  
 346 presence of multiple protonated complexes. Thus, the definition of  $\beta^{\text{app}}$  in Eq. 20 can be expressed  
 347 in terms of the individual Pu(IV)-CDTA stability constants as [45-47]:

$$\beta^{\text{app}} \left(1 + \sum \beta_{1-h0} [\text{H}^+]^h\right) = \beta_{101} + \beta_{111} [\text{H}^+] + \beta_{121} [\text{H}^+]^2 \quad (21)$$

348 The values of  $\beta_{101}$ ,  $\beta_{111}$ , and  $\beta_{121}$  were determined from the coefficients of the 2<sup>nd</sup>-order polynomial  
 349 fit and are listed in Table 4.

350 An aqueous Pu(IV)-CDTA speciation plot (Fig. 8) was developed, using the acid  
351 dissociation constants and stability constants determined in this work and the Pu(IV) hydrolysis  
352 constants from Baes and Mesmer [38]. The modeling conditions reflect the solution conditions  
353 that were used in the liquid-liquid extraction experiments from which the stability constants were  
354 measured, and therefore only a  $pC_H$  range of -1 to 3 was modeled to remain representative of the  
355 acidic conditions explored in the experiments. According to the speciation model, the protonated  
356 Pu(IV)-CDTA complexes start to form at  $pC_H \sim 0$ . Initially, we attempted to determine the stability  
357 constants in  $1.00 \text{ mol}\cdot\text{L}^{-1} \text{ HClO}_4$  (i.e.  $pC_H = 0$ ) but we did not observe any changes in the  
358 distribution ratio with varied CDTA concentration. This observation was an indication that no  
359 Pu(IV)-CDTA complexation was occurring under these conditions and indeed matches what is  
360 predicted by the speciation model. There is a mixture of the protonated complexes  $\text{Pu}(\text{H}_2\text{CDTA})^{2+}$   
361 and  $\text{Pu}(\text{HCDTA})^+$  between  $pC_H$  0 and 1, where  $\text{Pu}(\text{HCDTA})^+$  becomes the primary Pu(IV) species  
362 at a  $pC_H$  of 0.8. The protonated complexes are deprotonated and disappear as the  $pC_H$  is increased,  
363 forming the 1:0:1 complex,  $\text{PuCDTA}^0$ , as the dominant Pu(IV) species at  $pC_H > 2$ . Of additional  
364 note, Pu(IV) is fully complexed upon reaching  $pC_H$  1 and the hydrolysis of Pu(IV) is effectively  
365 suppressed when CDTA is in stoichiometric excess.

366 The only other reported study of Pu complexation with CDTA was a potentiometric study  
367 of Pu(III), and the reported stability constant for the Pu(III)-CDTA complex was  
368  $\log_{10} \beta_{101} = 17.70 \pm 0.02$  ( $1 \text{ mol}\cdot\text{L}^{-1} \text{ KCl}$ ,  $25.00 \pm 0.01^\circ\text{C}$ ) [13]. The greater value of  
369  $\log_{10} \beta_{101} = 24.2 \pm 0.3$  ( $1.00 \text{ mol}\cdot\text{L}^{-1} (\text{Na},\text{H})\text{ClO}_4$ ,  $23 \pm 1^\circ\text{C}$ ) we obtained for the Pu(IV)-CDTA  
370 system follows the expected trend of increasing complexation strength on the order of  
371  $\text{Pu(III)} < \text{Pu(IV)}$ , due to the increased cationic charge and Lewis acidity of Pu(IV) compared to  
372 Pu(III). While no other Pu(IV)-CDTA studies have been reported, comparisons to Pu(IV)-EDTA

373 complexes can be informative due to the similar structures of the two ligands. Foreman et al. [9]  
374 calculated a Pu(IV)-EDTA stability constant of  $\log_{10} \beta_{101} = 24.2$  in  $1 \text{ mol}\cdot\text{L}^{-1}$   $\text{HNO}_3$  with  
375 spectrophotometry and Cauchetier et al. [10] report  $\log_{10} \beta_{101} = 25.6$  in  $0.1 \text{ mol}\cdot\text{L}^{-1}$  ionic strength  
376 of unspecified background electrolyte. Using a liquid-liquid extraction method, Thakur et al. [11]  
377 report  $\log_{10} \beta_{101} = 24.55 \pm 0.22$  from an acidic solution of  $1.0 \text{ mol}\cdot\text{L}^{-1}$   $\text{HClO}_4/4.0 \text{ mol}\cdot\text{L}^{-1}$   $\text{NaClO}_4$   
378 and  $25^\circ\text{C}$  but did not report any protonated complexes as they did not perform experiments at  
379 varied acid concentration, which is necessary in order to observe those complexes. Perhaps the  
380 most complete study of Pu(IV)-EDTA solution equilibria was performed by Boukhalfa et al. [12]  
381 who utilized potentiometry, spectrophotometry, and cyclic voltammetry to identify Pu(IV)-EDTA  
382 and ternary mixed-ligand complexes in solution. At a 1:1 metal to ligand ratio they found the 1:0:1  
383 complex,  $\text{PuEDTA}^0$ , to dominate in acidic solutions of  $\text{pH} < 4$  ( $\log_{10} \beta_{101} = 26.44 \pm 0.20$ ,  
384  $1.0 \text{ mol}\cdot\text{L}^{-1}$   $\text{NaClO}_4$ ,  $25^\circ\text{C}$ ), followed by the formation of hydroxo species at higher pH. When  
385 they changed the metal to ligand ratio to 1:2, they observed the formation of bis-EDTA complexes  
386 with Pu(IV) at near neutral pH, where the  $\text{PuEDTA}^0$  species was still the dominant complex under  
387 acidic pH. In our experiments CDTA was present in great stoichiometric excess relative to Pu(IV),  
388 but it is unlikely that similar bis-CDTA complexes would form under the acidic conditions of  
389  $0.10\text{--}0.50 \text{ mol}\cdot\text{L}^{-1}$   $\text{HClO}_4$  studied, as was the case for the Pu(IV)-EDTA system.

390 Metal-ligand complex stability constants of EDTA and CDTA generally increase in the  
391 order EDTA < CDTA. This is indeed the case for other tetravalent cations, such as Th(IV), for  
392 which  $\log_{10} \beta_{101}$  values of 22.3 with EDTA and 24.5 with CDTA ( $0.5 \text{ mol}\cdot\text{L}^{-1}$   $\text{Na}^+$  salt,  
393  $25^\circ\text{C}$ ) were reported [27]. This free energy relationship can be attributed to two factors: (1) the  
394 increase in total basicity ( $\Sigma pK_a$ ) of CDTA ( $\Sigma pK_a = 23.5 \pm 0.2$ ,  $1.00 \text{ mol}\cdot\text{L}^{-1}$   $\text{NaClO}_4$ , present work)  
395 compared to EDTA ( $\Sigma pK_a = 20.9 \pm 0.3$ ,  $1.0 \text{ mol}\cdot\text{L}^{-1}$   $\text{NaClO}_4$ , [27]), and (2) a thermodynamic

396 effect where the carboxylate groups on CDTA are pre-organized in an orientation appropriate for  
397 binding a metal cation because of its rigid cyclohexane backbone, while the more flexible EDTA  
398 molecule has an energy cost associated with orienting the ligand into the required binding  
399 geometry. Regarding the second reason, the stronger metal-ligand complexes with CDTA would  
400 likely be represented thermodynamically by having a more favorable change in the reaction  
401 entropy compared with EDTA complexes. Therefore, we anticipated a larger  $\beta_{101}$  for  
402 Pu(IV)-CDTA than for Pu(IV)-EDTA based on this free energy relationship. Yet, our value of  
403  $\beta_{101}$  for Pu(IV)-CDTA is slightly lower than the aforementioned values reported for Pu(IV)-EDTA.  
404 However, the absence of protonated Pu(IV)-EDTA species in the literature, which likely do form  
405 under the acidic conditions that were studied, could result in inaccurately high values of  $\beta_{101}^{\text{EDTA}}$ ,  
406 explaining this apparent non-congruence. A comprehensive study of Pu(IV) complexes with  
407 EDTA and CDTA at varied temperatures would be beneficial to better understand the underlying  
408 thermodynamics of these systems and provide a better understanding of the similarities and  
409 differences between these two systems.

410 **Acknowledgements**

411 This work was funded by the U.S. National Nuclear Security Administration, under the  
412 SSAA Grant DE-NA0002916 and by the U.S. Department of Energy Nuclear Energy University  
413 Program (NEUP) through grant DE-NE0000674. The portion of the work involving the use of Pu  
414 was performed in the Glenn T. Seaborg Institute at Lawrence Livermore National Laboratory  
415 (LLNL) under the Academic Cooperation Program and work was performed under the auspices of  
416 the U.S. Department of Energy by Lawrence Livermore National Laboratory under Contract DE-  
417 AC52-07NA27344. The authors thank Dr. James Begg (LLNL), Dr. Enrica Balboni (LLNL), and  
418 Dr. Nicholas Travia (LLNL) for their assistance and support in facilitating this work.

419 **Conflict of Interest**

420 The authors declare no conflict of interest.

421 **References**

- 422 1. Sypula, M., Wilden, A., Schreinemachers, C., Malmbeck, R., Geist, A., Taylor, R., Modolo, G.: Use of Polyaminocarboxylic Acids as Hydrophilic Masking Agents for Fission Products in Actinide Partitioning Processes. *Solvent Extr. Ion Exch.* **30** 748-764 (2012)
- 423 2. Liljenzin, J.O., Rydberg, J., Skarnemark, G.: Reducing the Long-Term Hazard of Reactor Waste Through Actinide Removal and Destruction in Nuclear Reactors. *Sep. Sci. Technol.* **15**, 799-824 (1980)
- 424 3. Mathur, J.N., Murali, M.S., Nash, K.L.: Actinide Partitioning—A Review. *Solvent Extr. Ion Exch.* **19**, 357-390 (2001)
- 425 4. Nilsson, M., Nash, K.L.: Review Article: A Review of the Development and Operational Characteristics of the TALSPEAK Process. *Solvent Extr. Ion Exch.* **25**, 665-701 (2007)
- 426 5. Gelis, A.V., Lumetta, G.J.: Actinide Lanthanide Separation Process—ALSEP. *Ind. Eng. Chem. Res.* **53**, 1624-1631 (2014)
- 427 6. Carrott, M., Geist, A., Hères, X., Lange, S., Malmbeck, R., Miguirditchian, M., Modolo, G., Wilden, A., Taylor, R.: Distribution of plutonium, americium and interfering fission products between nitric acid and a mixed organic phase of TODGA and DMDOHEMA in kerosene, and implications for the design of the "EURO-GANEX" process. *Hydrometallurgy* **152**, 139-148 (2015)
- 428 7. Rai, D., Bolton, H., Moore, D.A., Hess, N.J., Choppin, G.R.: Thermodynamic model for the solubility of  $\text{PuO}_2(\text{am})$  in the aqueous  $\text{Na}^+ \text{-} \text{H}^+ \text{-} \text{OH}^- \text{-} \text{Cl}^- \text{-} \text{H}_2\text{O}$ -ethylenediaminetetraacetate system. *Radiochim. Acta* **89**, 67-74 (2001)
- 429 8. Foreman, J.K., Smith, T.D.: The Nature and Stability of the Complex Ions formed by Ter-, Quadri-, and Sexa-valent Plutonium Ions with Ethylenediaminetetraacetic Acid. Part I. pH Titrations and Ion-exchange Studies. *J. Chem. Soc.* **1**, 1752-1758 (1957)
- 430 9. Foreman, J.K., Smith, T.D.: The Nature and Stability of the Complex Ions formed by Ter-, Quadri-, and Sexa-valent Plutonium Ions with Ethylenediaminetetraacetic Acid (edta). Part II. Spectrophotometric Studies. *J. Chem. Soc.* **1**, 1758-1762 (1957)
- 431 10. Cauchetier, P., Guichard, C.: Etude électrochimique et spectrophotométrique des complexes des ions du plutonium avec l'EDTA. *Radiochim. Acta* **19**, 137-146 (1973)

460 11. Thakur, P., Pathak, P.N., Choppin, G.R.: Complexation thermodynamics and the formation of  
461 the binary and the ternary complexes of tetravalent plutonium with carboxylate and  
462 aminocarboxylate ligands in aqueous solution of high ionic strength. *Inorg. Chim. Acta* **362**,  
463 179-184 (2009)

464

465 12. Boukhalfa, H., Reilly, S.D., Smith, W.H., Neu, M.P.: EDTA and Mixed-Ligand Complexes of  
466 Tetravalent and Trivalent Plutonium. *Inorg. Chem.* **43**, 5816-5823 (2004)

467

468 13. Merciny, E., Gatez, J.M., Duyckaerts, G.: Constants de formation des complexes de  
469 stoechiometrie 1:1 et 1:2 ainsi que des complexes mixtes formes entre le plutonium(III) et  
470 divers acides amino-polyacétiques. *Anal. Chim. Acta* **100**, 329-342 (1978)

471

472 14. Gans, P., O'Sullivan, B.: GLEE, a new computer program for glass electrode calibration.  
473 *Talanta* **51**, 33-37 (2000)

474

475 15. Gans, P.: GLEE: GLass Electrode Evaluation, Ver. 3.0.21; Protonic Software: 2 Templegate  
476 Avenue, Leeds LS15 0HD, England (2007)

477

478 16. Boggs, M.A., Mason, H., Arai, Y., Powell, B.A., Kersting, A.B., Zavarin, M.: Nuclear  
479 Magnetic Resonance Spectroscopy of Aqueous Plutonium(IV) Desferrioxamine B Complexes.  
480 *Eur. J. Inorg. Chem.* 3312-3321 (2014)

481

482 17. Begg, J.D., Zavarin, M., Tumey, S.J., Kersting, A.B.: Plutonium sorption and desorption  
483 behavior on bentonite. *J. Environ. Radioact.* **141**, 106-114 (2015)

484

485 18. Neu, M.P., Hoffman, D C., Roberts, K.E., Nitsche, H., Silva, R.J.: Comparison of Chemical  
486 Extractions and Laser Photoacoustic Spectroscopy for the Determination of Plutonium Species  
487 in Near-Neutral Carbonate Solutions. *Radiochim. Acta* **66/67**, 251-258 (1994)

488

489 19. Zhao, P., Begg, J.D., Zavarin, M., Tumey, S.J., Williams, R., Dai, Z.R., Kips, R., Kersting,  
490 A.B.: Plutonium(IV) and (V) Sorption to Goethite at Sub-Femtomolar to Micromolar  
491 Concentrations: Redox Transformations and Surface Precipitation. *Environ. Sci. Technol.* **50**,  
492 6948-6956 (2016)

493

494 20. Gran, G.: Determination of the Equivalence Point in Potentiometric Titrations. Part II. *Analyst*  
495 **77**, 661-671 (1952)

496

497 21. Gans, P., Sabatini, A., Vacca, A.: Investigation of equilibria in solution. Determination of  
498 equilibrium constants with the HYPERQUAD suite of programs. *Talanta* **43**, 1739-1753  
499 (1996)

500

501 22. Gans, P., Sabatini, A., Vacca, A.: Hyperquad2013, Ver. 6.0.1; Protonic Software: 2  
502 Templegate Avenue, Leeds LS15 0HD, England (2013)

503

504 23. Rossotti, F.J.C., Rossotti, H.: Chapter 7. Potentiometry. In: Rossotti, F.J.C., Rossotti, H. (eds.)  
505 The Determination of Stability Constants and Other Equilibrium Constants in Solution, pp  
506 127-170. McGraw-Hill Book Company, Inc., New York (1961)

507

508 24. Glab, S., Hulanicki, A.: Autoprotolysis Constants by Coulometric Titration. *Talanta* **28**, 183-  
509 186 (1981)

510

511 25. Gonzalez, A.G., Pablos, F.: Evaluation of acidity constants in dioxane-water mixtures by  
512 spectrophotometric and potentiometric pH titrations. *Anal. Chim. Acta* **251**, 321-325 (1991)

513

514 26. Felmy, H.M., Bennett, K.T., Clark, S.B.: The impact of mixed solvents on the complexation  
515 thermodynamics of Eu(III) by simple carboxylate and amino carboxylate ligands. *J. Chem.*  
516 *Thermodynamics* **114**, 83-92 (2017)

517

518 27. Smith, R.M., Martell, A., Motekaitis, R.: NIST Critically Selected Stability Constants of Metal  
519 Complexes Database, Ver. 8.0; NIST Standard Reference Database 46, National Institute of  
520 Standards and Technology (2004)

521

522 28. Fanghänel, T., Neck, V., Kim, J.I.: The Ion Product of H<sub>2</sub>O, Dissociation Constants of H<sub>2</sub>CO<sub>3</sub>  
523 and Pitzer Parameters in the System Na<sup>+</sup>/H<sup>+</sup>/OH<sup>-</sup>/HCO<sub>3</sub><sup>-</sup>/CO<sub>3</sub><sup>2-</sup>/ClO<sub>4</sub><sup>-</sup>/H<sub>2</sub>O at 25 °C. *J.*  
524 *Solution Chem.* **25**, 327-343 (1996)

525

526 29. Du, M., Choppin, G.R.: Correlation of Equilibrium Constants with Ionic Strength by SIT,  
527 Pitzer and Parabolic Models. In: Reed, D.T., Clark, S.B., Rao, L. (eds.) *Actinide Speciation in*  
528 *High Ionic Strength Media*, pp 125-139. Springer, New York (1999)

529

530 30. Bernardo, P.D., Zanonato, P., Bismundo, A., Jiang, H., Garnov, A.Y., Jiang, J., Rao, L.:  
531 Complexation of Uranium(VI) with Thiodiacetic Acid in Solution at 10-85 °C. *Eur. J. Inorg.*  
532 *Chem.* **45** 33-4540 (2006)

533

534 31. Lagerström, G.: Equilibrium Studies of Polyanions III. Silicate Ions in NaClO<sub>4</sub> Medium. *Acta*  
535 *Chem. Scand.* **13**, 722-736 (1959)

536

537 32. Chinea, E., Domínguez, S., Mederos, A., Brito, F., Arrieta, J.M., Sánchez, A., Germain, G.:  
538 Nitrilotripropionic Acid (NTP) and Other Polyamino Carboxylic Acids as Sequestering  
539 Agents for Beryllium(II). X-ray Crystal Structure of Sodium (Nitrilotripropionato)beryllate(II)  
540 Trihydrate, Na[Be(NTP)<sub>3</sub>]<sub>2</sub>·3H<sub>2</sub>O. *Inorg. Chem.* **34**, 1579-1587 (1995)

541

542 33. Anderegg, G.: Komplexone XL. Die Protonierungskonstanten einiger Komplexone in  
543 verschiedenen wässrigen Salzmedien (NaClO<sub>4</sub>, (CH<sub>3</sub>)<sub>4</sub>NCl, KNO<sub>3</sub>). *Helv. Chim. Acta* **50**,  
544 2333-2340 (1967)

545

546 34. Kragten, J., Decnop-Weever, L.G.: Solubility and protonation of EDTA, DCTA and DPTA in  
547 acidic perchlorate medium. *Talanta* **30**, 623-626 (1983)

548

549 35. Beck, M.T., Görög, S.: Water solubility of ethylenediamine and cyclohexandiaminetetraacetic  
550 acid as a function of acidity. *Chemist Analyst* **48**, 90-91 (1959)

551

552 36. Hummel, W., Anderegg, G., Puigdomènech, I., Rao, L., Tochiyama, O.: Chemical  
553 Thermodynamics of Compounds and Complexes of U, Np, Pu, Am, Tc, Se, Ni, and Zr with  
554 Selected Organic Ligands. In: OECD Nuclear Energy Agency (ed.), *Chemical  
555 Thermodynamics*, Vol. 9, Elsevier, New York (2005)

556

557 37. Connick, R.E., McVey, W.H.: The Aqueous Chemistry of Zirconium. *J. Am. Chem. Soc.* **71**,  
558 3182-3191 (1949)

559

560 38. Baes, C.F., Mesmer, R.E.: In: Baes, C.F., Mesmer, R.E. (eds.) *The Hydrolysis of Cations*, pp.  
561 174-191. John Wiley & Sons Inc., New York (1976)

562

563 39. Xia, Y.X., Friese, J.I., Moore, D.A., Bachelor, P.P., Rao, L.: Complexation of plutonium(IV)  
564 with sulfate at variable temperatures. *J. Radioanal. Nucl. Chem.* **274**, 79-86 (2007)

565

566 40. Xia, Y., Rao, L., Friese, J.I., Moore, D.A., Bachelor, P.P.: Complexation of plutonium(IV)  
567 with fluoride at variable temperatures. *Radiochim. Acta* **98**, 65-69 (2010)

568

569 41. Poskanzer, A.M., Foreman, B.M.L A summary of TTA extraction coefficients. *J. Inorg. Nucl.  
570 Chem.* **16**, 323-336 (1961)

571

572 42. Ramakrishna, V.V., Patil, S.K., Prakas, B.H.: Solvent Extraction and Spectrophotometric  
573 Studies on Synergistic Extraction of Plutonium(IV) by Mixtures of Thenoyltrifluoroacetone  
574 (HTTA) and Tri-*n*-butylphosphate (TBP) in Benzene. *Sep. Sci. Technol.* **14**, 571-589 (1979)

575

576 43. Nash, K.L., Cleveland, J.M.: Free Energy, Enthalpy, and Entropy of Plutonium(IV)-Sulfate  
577 Complexes. *Radiochim. Acta* **33**, 105-111 (1983)

578

579 44. El-Hefny, N.E., El-Nadi, Y.A., Daoud, J.A.: Effect of Diluents on the Extraction of Zirconium  
580 from Nitrate Medium by Thenoyltrifluoroacetone. *Solvent Extr. Ion Exch.* **25**, 703-717 (2006)

581

582 45. Shanbhag, S.M., Choppin, G.R.: Determination of the Stability Constant for MHL Formation  
583 by a Tracer Method. *Inorg. Chem.* **21**, 1697-1698 (1982)

584

585 46. Pokrovsky, O.S., Bronikowski, M.G., Moore, R.C., Choppin, G.R.: Interaction of Neptunyl(V)  
586 and Uranyl(VI) with EDTA in NaCl Media: Experimental Study and Pitzer Modeling.  
587 *Radiochim. Acta* **80**, 23-29 (1998)

588

589 47. Jensen, M.P., Chiarizia, R., Shkrob, I.A., Ulicki, J.S., Spindler, B.D., Murphy, D.J., Hossain,  
590 M., Roca-Sabio, A., Platas-Iglesias, C., de Blas, A., Rodríguez-Blas, T.: Aqueous Complexes  
591 for Efficient Size-based Separation of Americium from Curium. *Inorg. Chem.* **53**, 6003-6012  
592 (2014)

593

**Table 1** Description of the materials used in this work

Material	Abbreviation	Source	Mass fraction purity <sup>a</sup>
AG 1-X8 anion exchange resin (100-200 mesh)		Bio-Rad Laboratories	
<i>trans</i> -1,2-Diaminocyclohexane- <i>N,N,N',N'</i> -tetraacetic acid monohydrate	H <sub>4</sub> CDTA·H <sub>2</sub> O	TCI	> 99.0%
Hydrochloric acid	HCl	BDH Chemicals	36.5-38.0%
Nitric acid	HNO <sub>3</sub>	BDH Chemicals	68-70%
Perchloric acid	HClO <sub>4</sub>	Alfa Aesar	70%
1-Phenyl-3-methyl-4-benzoyl-2-pyrazolin-5-one	PMBP	Sigma-Aldrich	99%
Potassium hydrogen phthalate	KHP	Acros Organics	> 99%
Sodium hydroxide (pellets)	NaOH	Fisher Scientific	≥ 97.0%
Sodium nitrite	NaNO <sub>2</sub>	J. T. Baker	99.6%
Sodium perchlorate (anhydrous)	NaClO <sub>4</sub>	Alfa Aesar	98.0-102.0%
Sodium perchlorate (monohydrate)	NaClO <sub>4</sub> ·H <sub>2</sub> O	Fluka Analytical	≥ 99.0%
2-Thenoyltrifluoroacetone	TTA	Sigma-Aldrich	99%
Ultima Gold LLT liquid scintillation cocktail		PerkinElmer	
<i>p</i> -Xylene		Acros Organics	99%

<sup>a</sup>Purities as provided by the supplier

**Table 2** Autoprotolysis of water and acid dissociation constants for CDTA in NaClO<sub>4</sub> media

Ionic strength	T (°C)	pK <sub>w</sub>	pK <sub>a1</sub>	pK <sub>a2</sub>	pK <sub>a3</sub>	pK <sub>a4</sub>	pK <sub>a5</sub>	pK <sub>a6</sub>	Ref.
0.10 mol·L <sup>-1</sup> NaClO <sub>4</sub>	25.0 ± 0.1	13.78 ± 0.02		1.6 ± 0.5	2.59 ± 0.07	3.72 ± 0.03	6.13 ± 0.02	9.80 ± 0.09	p.w. <sup>a</sup>
0.10 mol·L <sup>-1</sup> Na <sup>+</sup> salt	25.0	13.78 ± 0.01			2.48 ± 0.08	3.50 ± 0.05	6.07 ± 0.02		27
0.10 mol·L <sup>-1</sup> NaClO <sub>4</sub>	25	13.79 ± 0.03							28
0.10 mol·L <sup>-1</sup> NaClO <sub>4</sub>	25	13.80 ± 0.02							29
0.50 mol·L <sup>-1</sup> NaClO <sub>4</sub>	25.0 ± 0.1	13.74 ± 0.02		1.6 ± 0.2	2.48 ± 0.04	3.41 ± 0.05	5.85 ± 0.05	9.35 ± 0.05	p.w.
0.50 mol·L <sup>-1</sup> Na <sup>+</sup> salt	25.0	13.73 ± 0.04						11.3	27
0.50 mol·L <sup>-1</sup> NaClO <sub>4</sub>	25	13.77 ± 0.01							29
0.50 mol·L <sup>-1</sup> NaClO <sub>4</sub>	25	13.73							31
0.50 mol·L <sup>-1</sup> NaClO <sub>4</sub>	25			1.91 ± 0.03	2.45 ± 0.02	3.35 ± 0.01	5.80 ± 0.02	9.31 ± 0.07	32
1.00 mol·L <sup>-1</sup> NaClO <sub>4</sub>	25.0 ± 0.1	13.76 ± 0.02		1.7 ± 0.1	2.46 ± 0.02	3.27 ± 0.04	5.86 ± 0.04	9.27 ± 0.04	p.w.
1.0 mol·L <sup>-1</sup> Na <sup>+</sup> salt	25.0	13.77 ± 0.04		1.6 ± 0.1	2.42 ± 0.01	3.21 ± 0.04	5.84	9.22	27
1.0 mol·L <sup>-1</sup> NaClO <sub>4</sub>	25	13.81 ± 0.04							28
1.0 mol·L <sup>-1</sup> NaClO <sub>4</sub>	25	13.82 ± 0.02							29
1.05 mol·kg <sup>-1</sup> NaClO <sub>4</sub>	25	13.78 ± 0.01							30
1.0 mol·L <sup>-1</sup> NaClO <sub>4</sub>	20	13.95		1.72	2.41	3.52	5.87	9.30	33
1.0 mol·L <sup>-1</sup> NaClO <sub>4</sub>	21			1.78 ± 0.02	2.30 ± 0.02	3.50 ± 0.03			34
Dilute HClO <sub>4</sub>	20		0.96	1.92					33, 35
1 mol·L <sup>-1</sup> KCl	25.00 ± 0.01		1.09 ± 0.02	1.68 ± 0.02	2.32 ± 0.01	3.18 ± 0.01	5.98 ± 0.01	12.13 ± 0.01	13
1.50 mol·L <sup>-1</sup> NaClO <sub>4</sub>	25.0 ± 0.1	13.82 ± 0.02							p.w.
2.00 mol·L <sup>-1</sup> NaClO <sub>4</sub>	25.0 ± 0.1	13.87 ± 0.03		1.9 ± 0.1	2.55 ± 0.07	3.02 ± 0.05	6.06 ± 0.04	9.31 ± 0.03	p.w.
2.0 mol·L <sup>-1</sup> NaClO <sub>4</sub>	25.0	13.95 ± 0.01							27

<sup>a</sup>p.w. = present work

The standard uncertainties are  $u(T) = 0.1$  °C. The expanded uncertainties are  $u(K_i) = K_i \cdot \sqrt{(3\sigma \cdot K_i^{-1})^2 + (u(T) \cdot T^{-1})^2}$  where  $\sigma$  is the standard deviation from replicates with  $n = 4$  (99% confidence level).

**Table 3** SIT parameters for the dissociation constants of water and CDTA from NaClO<sub>4</sub> media at 25.0 ± 0.1 °C

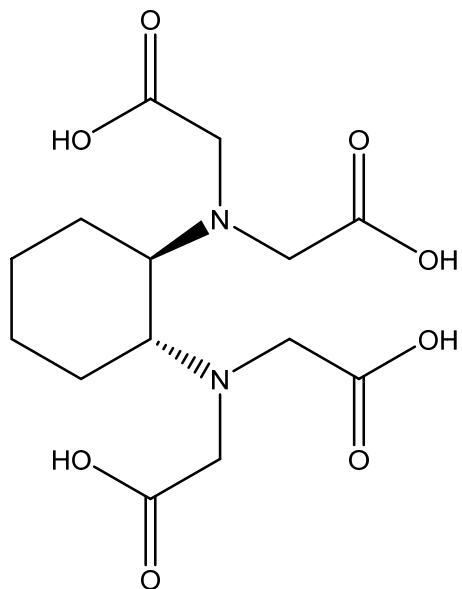
Ionic strength (mol·L <sup>-1</sup> )	$\vartheta$ (L·kg <sup>-1</sup> ) <sup>a</sup>	$a_{H_2O}$ <sup>a</sup>	Constant	Value	$\Delta z^2$	$\Delta \varepsilon$ (kg·mol <sup>-1</sup> )	Ref.
0.10	1.0075	0.9966	$pK_w^\circ$	14.00 ± 0.04	2	0.13 ± 0.02	p.w. <sup>b</sup>
0.50	1.0265	0.9833		13.997 ± 0.003			27
1.00	1.0515	0.9660		14.013	2	0.1910	29
1.50	1.0780	0.9476		$pK_{a1}^\circ$			
2.00	1.1062	0.9279		$pK_{a2}^\circ$	0	0.15 ± 0.03	p.w.
				$pK_{a3}^\circ$	2	0.07 ± 0.05	p.w.
				$pK_{a4}^\circ$	4	-0.11 ± 0.03	p.w.
				$pK_{a5}^\circ$	6	0.30 ± 0.01	p.w.
				$pK_{a6}^\circ$	8	0.23 ± 0.02	p.w.

601 <sup>a</sup>From Ref. [36]602 <sup>b</sup>p.w. = present work603 The standard uncertainties are  $u(T) = 0.1$  °C. The expanded uncertainties are  $u(K_i^\circ) = K_i^\circ \cdot \sqrt{(3\sigma \cdot K_i^{\circ-1})^2 + (u(T) \cdot T^1)^2}$  and604  $u(\Delta \varepsilon) = \Delta \varepsilon \cdot \sqrt{(3\sigma \cdot \Delta \varepsilon^{-1})^2 + (u(T) \cdot T^1)^2}$  where  $\sigma$  is the standard deviation from replicates with  $n = 4$  (99% confidence level).

605 **Table 4** Equilibrium constants for the liquid-liquid extraction of Pu(IV) with TTA and complexation reactions with CDTA

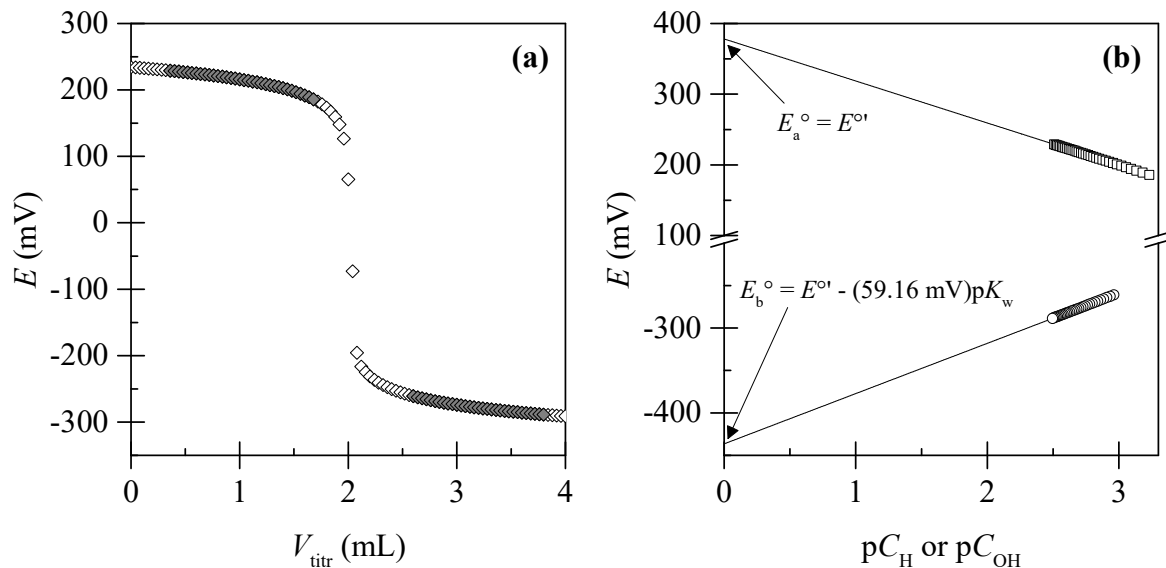
Reaction	Medium	T (°C)	Constant	Value	Ref.
$\text{Pu}^{4+} + 4\text{HTTA}_{(\text{org})} \rightleftharpoons \text{Pu}(\text{TTA})_4 \text{ (org)} + 4\text{H}^+$	1.00 mol·L <sup>-1</sup> (Na,H)ClO <sub>4</sub> / <i>p</i> -xylene	23 ± 1	$\log_{10} K_{\text{ex}}$	6.02 ± 0.06	p.w. <sup>a</sup>
	1 mol·L <sup>-1</sup> HClO <sub>4</sub> /benzene			6.8	41
	1.0-2.0 mol·L <sup>-1</sup> HClO <sub>4</sub> /benzene	25		7.3	42
	2.0 mol·L <sup>-1</sup> (Na,H)ClO <sub>4</sub> /toluene	25.0		6.6 ± 0.1	43
	2.0 mol·L <sup>-1</sup> HClO <sub>4</sub> /toluene	25		7.08 ± 0.01	39, 40
$\text{Pu}^{4+} + \text{CDTA}^{4-} \rightleftharpoons \text{PuCDTA}^0$	1.00 mol·L <sup>-1</sup> (Na,H)ClO <sub>4</sub>	23 ± 1	$\log_{10} \beta_{101}$	24.2 ± 0.3	p.w.
$\text{Pu}^{4+} + \text{H}^+ + \text{CDTA}^{4-} \rightleftharpoons \text{Pu}(\text{HCDTA})^+$	1.00 mol·L <sup>-1</sup> (Na,H)ClO <sub>4</sub>	23 ± 1	$\log_{10} \beta_{111}$	25.4 ± 0.2	p.w.
$\text{Pu}^{4+} + 2\text{H}^+ + \text{CDTA}^{4-} \rightleftharpoons \text{Pu}(\text{H}_2\text{CDTA})^{2+}$	1.00 mol·L <sup>-1</sup> (Na,H)ClO <sub>4</sub>	23 ± 1	$\log_{10} \beta_{121}$	25.8 ± 0.1	p.w.

606 <sup>a</sup>p.w. = present work607 The standard uncertainties are  $u(T) = 1$  °C. The expanded uncertainties are  $u(K_{\text{ex}}) = K_{\text{ex}} \cdot \sqrt{(2\sigma \cdot K_{\text{ex}}^{-1})^2 + (u(T) \cdot T^1)^2}$  and608  $u(\beta) = \beta \cdot \sqrt{(2\sigma \cdot \beta^{-1})^2 + (u(T) \cdot T^1)^2}$  where  $\sigma$  is the standard deviation from replicates with  $n = 3$  (95% confidence level).



609  
610

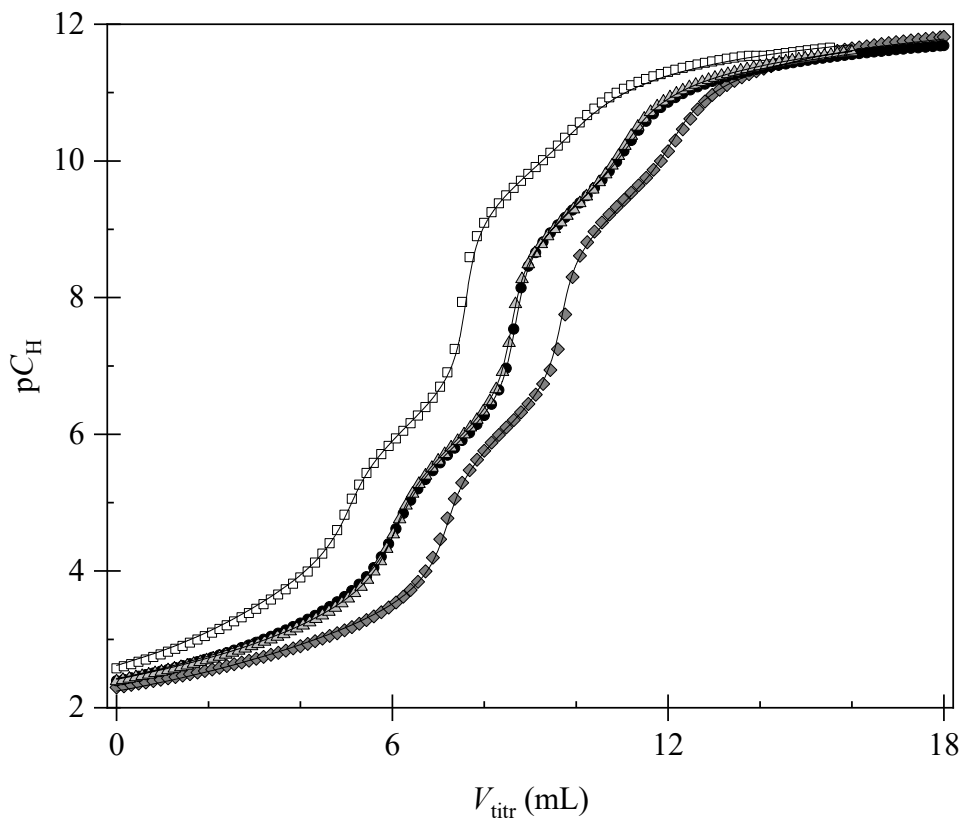
611 **Fig. 1** Chemical structure of *trans*-1,2-diaminocyclohexane-*N,N,N',N'*-tetraacetic acid (CDTA)



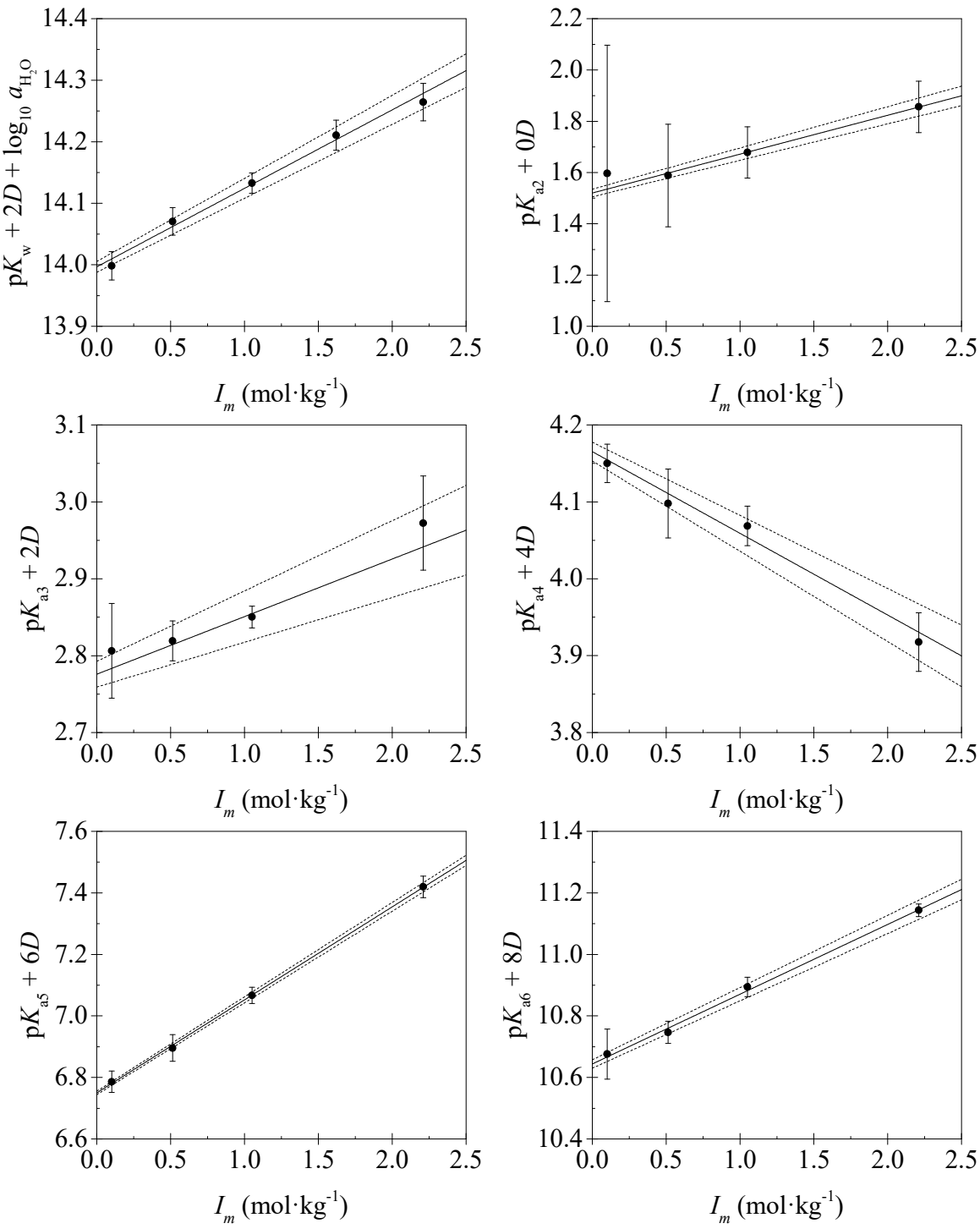
612  
613

614 **Fig. 2** (a) Gran titration plot used for electrode calibration at  $1.00 \text{ mol}\cdot\text{L}^{-1}$   $\text{NaClO}_4$  and  
615  $25.0 \pm 0.1^\circ\text{C}$ . Titrant:  $0.1000 \text{ mol}\cdot\text{L}^{-1}$   $\text{NaOH}/0.90 \text{ mol}\cdot\text{L}^{-1}$   $\text{NaClO}_4$ . Titrand:  $2.000 \text{ mL}$  of  
616  $0.1000 \text{ mol}\cdot\text{L}^{-1}$   $\text{HClO}_4/0.90 \text{ mol}\cdot\text{L}^{-1}$   $\text{NaClO}_4$  added to  $50.00 \text{ mL}$  of  $1.00 \text{ mol}\cdot\text{L}^{-1}$   $\text{NaClO}_4$ . The  
617 shaded data points were used to construct the plots in (b) for the determination of  $pK_w$ . In this  
618 example,  $E_a^\circ = 387.2 \pm 0.2 \text{ mV}$  and  $E_b^\circ = -436.5 \pm 0.2 \text{ mV}$ , giving a  $pK_w$  value of  $13.77 \pm 0.01$   
619 using Eq. 4.

620

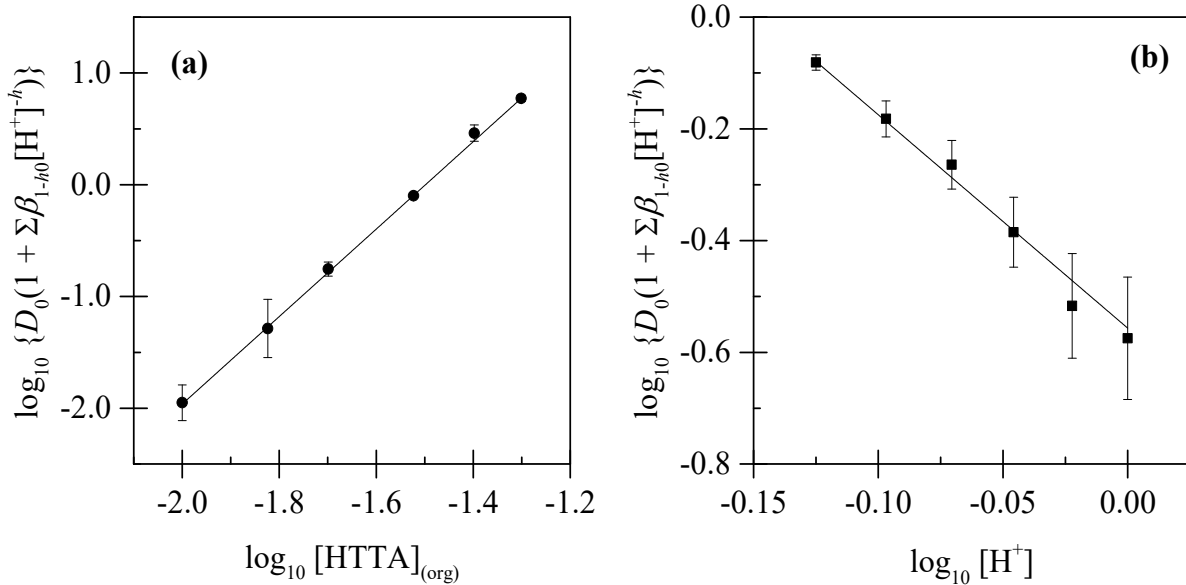


621  
 622 **Fig. 3** Titration curves of CDTA at  $0.10 \text{ mol}\cdot\text{L}^{-1}$  ( $\square$ ),  $0.50 \text{ mol}\cdot\text{L}^{-1}$  ( $\bullet$ ),  $1.00 \text{ mol}\cdot\text{L}^{-1}$  ( $\Delta$ ), and  
 623  $2.00 \text{ mol}\cdot\text{L}^{-1}$  ( $\blacklozenge$ )  $\text{NaClO}_4$  ionic strength and  $25.0 \pm 0.1 \text{ }^\circ\text{C}$ . Titrand:  $50.00 \text{ mL}$  of  
 624  $5.00 \times 10^{-3} \text{ mol}\cdot\text{L}^{-1}$  CDTA/ $\text{NaClO}_4$ . Titrant:  $0.1000 \text{ mol}\cdot\text{L}^{-1}$   $\text{NaOH}/\text{NaClO}_4$ . Data points  
 625 represent experimental data and solid lines are the calculated fits using the  $\text{p}K_w$  and  $\text{p}K_a$  values  
 626 presented in Table 2



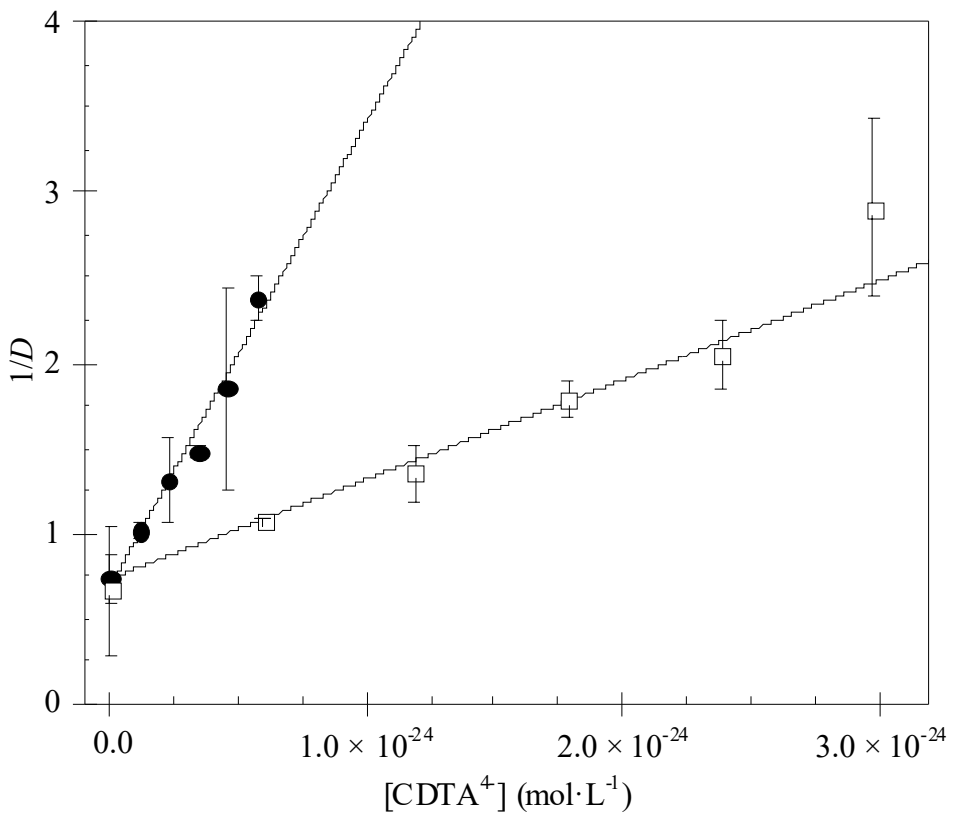
627  
628  
629  
630  
631

**Fig. 4** SIT plots of  $pK_w$  and CDTA  $pK_{ai}$  vs.  $I_m$  (molal scale) in  $\text{NaClO}_4$  media at  $25.0 \pm 0.1^\circ\text{C}$ . Error bars represent  $\pm 3\sigma$  from replicates ( $n = 4$ ). Solid lines are the error weighted linear fits obtained using Eqs. 7 or 8, while dashed lines represent the error limits obtained from the error weighted least squares regression



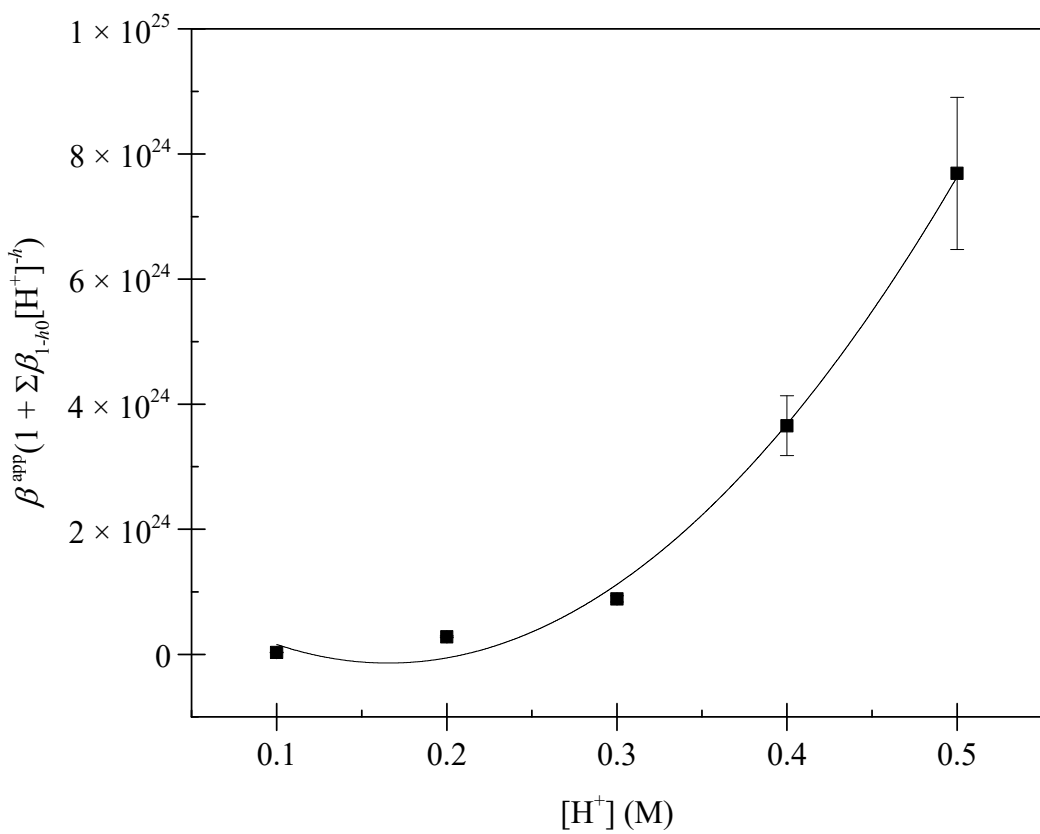
632  
633  
634  
635  
636  
637

**Fig. 5** Slope-analysis plots for the extraction of Pu(IV) from  $1.00 \text{ mol}\cdot\text{L}^{-1}$   $(\text{Na},\text{H})\text{ClO}_4$  with TTA in *p*-xylene at  $23 \pm 1$   $^\circ\text{C}$ . Error bars represent  $\pm 2\sigma$  from replicates ( $n = 3$ ). **(a)** TTA dependence:  $^{238}\text{Pu}(\text{IV})/1.00 \text{ mol}\cdot\text{L}^{-1} \text{ HClO}_4/0.010\text{--}0.050 \text{ mol}\cdot\text{L}^{-1} \text{ TTA}/p\text{-xylene}$ . Slope =  $3.9 \pm 0.1$ . **(b)**  $\text{H}^+$  dependence:  $^{238}\text{Pu}(\text{IV})/0.75\text{--}1.00 \text{ mol}\cdot\text{L}^{-1} \text{ HClO}_4/\text{NaClO}_4/0.030 \text{ mol}\cdot\text{L}^{-1} \text{ TTA}/p\text{-xylene}$ . Slope =  $-3.8 \pm 0.2$



638  
639  
640  
641  
642  
643  
644

**Fig. 6** Representative plots of  $1/D$  vs.  $[CDTA^{4-}]$  from the extraction system of  $^{238}\text{Pu}(\text{IV})/1.00 \text{ mol}\cdot\text{L}^{-1} (\text{Na},\text{H})\text{ClO}_4/0.020 \text{ mol}\cdot\text{L}^{-1} \text{ TTA}/p\text{-xylene}/23 \pm 1 \text{ }^\circ\text{C}$ , at acidities of  $0.40 \text{ mol}\cdot\text{L}^{-1} \text{ HClO}_4$  (●) and  $0.30 \text{ mol}\cdot\text{L}^{-1} \text{ HClO}_4$  (□). Error bars represent  $\pm 2\sigma$  from replicates ( $n = 3$ ). The value of  $1/D_0$  is obtained from the  $y$ -intercepts and the slopes are proportional to  $\beta^{\text{app}}$  from the error weighted least squares fitting. The changes in slope at different acidities indicate the presence of protonated Pu(IV)-CDTA complexes



645  
646 **Fig. 7** Variation in the hydrolysis corrected, apparent stability constants of Pu(IV)-CDTA with  
647  $[\text{H}^+]$  at a total ionic strength of  $1.00 \text{ mol}\cdot\text{L}^{-1}$  ( $\text{Na}_2\text{H}\text{ClO}_4$ ) and  $23 \pm 1 \text{ }^\circ\text{C}$ . Error bars represent  $\pm 2\sigma$   
648 from replicates ( $n = 3$ ). This data can be found in the supplementary material (Table S6)

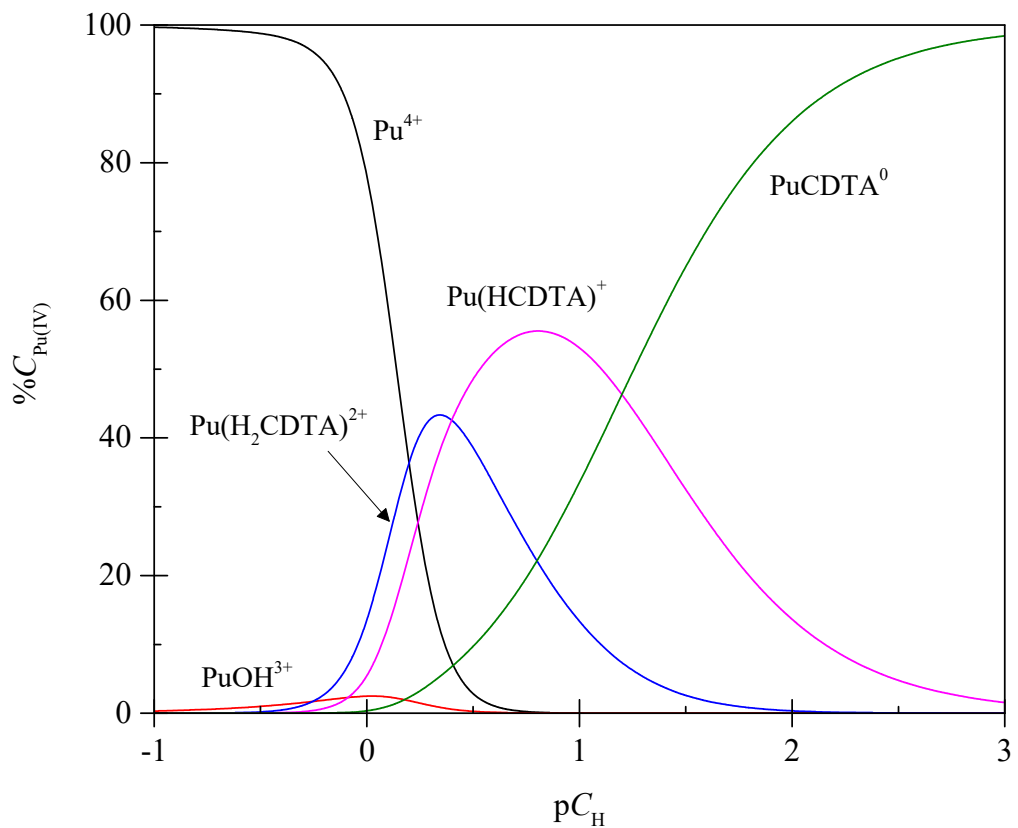


**Fig. 8** Pu(IV)-CDTA speciation diagram constructed using  $[\text{Pu(IV)}] = 5 \times 10^{-8} \text{ mol}\cdot\text{L}^{-1}$ ,  $[\text{CDTA}] = 1 \times 10^{-3} \text{ mol}\cdot\text{L}^{-1}$ , and the stability constants reported in this work at  $1.00 \text{ mol}\cdot\text{L}^{-1}$   $(\text{Na,H})\text{ClO}_4$  and  $23 \pm 1^\circ\text{C}$